AWARD NUMBER: W81XWH-13-1-0099

TITLE: **A Hybrid Neuromechanical Ambulatory Assist System**

PRINCIPAL INVESTIGATOR: Ronald J Triolo, Ph.D.

CONTRACTING ORGANIZATION: Case Western Reserve University
Cleveland, OH 44106

REPORT DATE: August 2016

TYPE OF REPORT: FINAL

PREPARED FOR: U.S. Army Medical Research and Materiel Command
Fort Detrick, Maryland 21702-5012

1. REPORT DATE	2. REPORT TYPE	3. DATES COVERED
August 2016	Final	15 May 2013 - 14 May 2016

4. TITLE AND SUBTITLE

A HYBRID NEUROMECHANICAL AMBULATORY ASSIST SYSTEM

5a. CONTRACT NUMBER

5b. GRANT NUMBER

W81XWH-13-1-0099

5c. PROGRAM ELEMENT NUMBER

6. AUTHOR(S)

Ronald J Triolo, PhD

E-Mail: Ronald.Triolo@case.edu

5d. PROJECT NUMBER

5e. TASK NUMBER

5f. WORK UNIT NUMBER

7. PERFORMING ORGANIZATION NAME(S) AND ADDRESS(ES)

Case Western Reserve University
10900 Euclid Ave.
Cleveland, OH 44106

8. PERFORMING ORGANIZATION REPORT NUMBER

9. SPONSORING / MONITORING AGENCY NAME(S) AND ADDRESS(ES)

U.S. Army Medical Research and Materiel Command
Fort Detrick, Maryland 21702-5012

10. SPONSOR/MONITOR'S ACRONYM(S)

11. SPONSOR/MONITOR'S REPORT NUMBER(S)

12. DISTRIBUTION / AVAILABILITY STATEMENT

Approved for Public Release; Distribution Unlimited

13. SUPPLEMENTARY NOTES

14. ABSTRACT

A hybrid neuromechanical ambulatory assist system was developed for walking after lower extremity paralysis that combines the stability and constraints of a novel hydraulic exoskeletal system with the mobility powered by the individual's own paralyzed muscles contracting via electrical stimulation. A mobile computing platform was designed to provide real-time closed-loop control using brace mounted sensors to deliver the stimulation needed to stand up and walk while coordinating exoskeletal control mechanisms at the hips and knees to maintain stability. A variable constraint hip mechanism couples hips as needed to maintain posture and reduces the need for upper extremities to maintain balance. The knee locking mechanism was designed to allow the stimulated muscles to rest during stance while permitting unconstrained movement during swing. A mechanical knee flexion assist was explored to provide sufficient foot clearance during swing on an uneven terrain. The exoskeleton was designed for easy fitting with adjustable uprights and hip abduction for donning for use in activities of daily living for persons with paraplegia. Future enhancements should include small motors at the hip and knee to provide assistive power in users with weakened or fatigued electrically stimulated muscles and stimulation of plantar flexors to provide push-off for forward progression.

15. SUBJECT TERMS

Exoskeleton, hydraulic, spinal cord injury, walking

16. SECURITY CLASSIFICATION OF:	17. LIMITATION OF ABSTRACT	18. NUMBER OF PAGES	19a. NAME OF RESPONSIBLE PERSON
			USAMRMC

a. REPORT	b. ABSTRACT	c. THIS PAGE			19b. TELEPHONE NUMBER *(include area code)*
Unclassified	Unclassified	Unclassified	Unclassified	31	

Standard Form 298 (Rev. 8-98)
Prescribed by ANSI Std. Z39.18

Table of Contents

INTRODUCTION

The first prototype of the Hybrid Neuroprosthesis (HNP1) shown in **Figure 1** for walking in paraplegia was a combination of controllable exoskeleton to stability, and neuromuscular electrical stimulation (NES) power joint movements by contracting the paralyzed muscles (Kobetic 2009). Hydraulic exoskeletal actuators enabled and disabled joint constraints for transition through the gait cycle. The HNP1 incorporated two mechanisms for control of the knees and hips – the dual state knee mechanism (DSKM) which locked the knee for stance and unlocked it for swing (To 2011), and the variable constraint hip mechanism (VCHM) which locked the hip for stance, unlocked it for swing or reciprocally coupled the two hips to maintain posture (To 2008). The HNP1 was controlled by an off board lab computer that read in sensor data, determined phases of gait, applied knee and hip joint constraints and modulated stimulation using a state based controller (To 2012, 2014). The evaluation in persons with paraplegia from spinal cord injury (SCI) showed that walking with the HNP1 significantly reduced the forward lean of NES-only walking and the maximum upper extremity forces for balance and support by 42 % and 19% as compared to an isocentric reciprocal gait orthosis (IRGO) and NES-only gait, respectively. The speed of walking with HNP1 was significantly faster than with IRGO and comparable to NES-only with less stimulation, thus potentially reducing muscle fatigue. Drawbacks of HNP1 were limited knee flexion in early swing to provide proper toe clearance for out of the lab use, weight of exoskeleton and lack of adjustability for fitting different users, and tethered to the lab-based computer, thus not conducive to evaluation for everyday use.

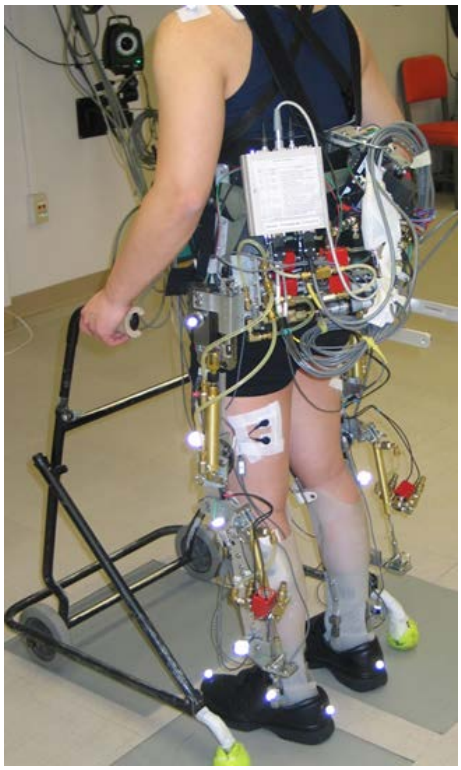

Figure 1. First generation hybrid neuroprosthesis (HNP1)

The purpose of this research project was to refine the design of the hybrid neuromechanical gait assist system that addresses drawbacks of the HNP1 and generate a prototype of a redesigned and refined second generation hybrid neuroprosthesis (HNP2) suitable for evaluation under real-world conditions outside of the laboratory environment.

NOTE: No human subject testing was supported by project W81XWH-13-1-0099, which focused exclusively the design, bench testing and production of the technical components of the untethered HNP2 prototype and new wireless communication and control system. Any human test results reported here were conducted under a separately funded project supported by the US Department of Veterans Affairs.

Keywords: exoskeleton, hydraulics, hybrid neuroprosthesis, electrical stimulation, spinal cord injury, walking

BODY

Work Accomplished under Statement of Work

Task 1 **– Design and implement new hydraulic hardware and control algorithms for synergistic coupling of hip and knee flexion during walking, including online adjustment of orthosis constraints and electrical stimulation.**

When using the HNP1, we were able to achieve sufficient hip flexion during swing phase of gait, but could not always achieve sufficient knee flexion especially in early swing. This resulted in inconsistent foot clearance during swing, leading to toe dragging and the inability to navigate uneven terrain. This motivated implementation of the hip-knee coupling (HKC) to enhance knee flexion by means of stimulation driven hip flexion, thus, decreasing the chance of toe dragging and increasing user safety during walking. Another advantage that hip-knee coupling could provide is to clear

the lip of the step during stair climbing. Without sufficient knee flexion, the leg gets caught on the lip and the user is unable to place the foot on the step above.

HKC Specifications

Able-bodied hip and knee joint angles during gait at slow cadence defined the HKC ratio of the hydraulic circuit (Winter 1991) (**Figure 2**, red shapes). The initial portion of swing phase (**Figure 2**, blue shapes with linear trend line) determined the required hip-knee joint angle ratio to be approximately 0.43°:1° or 1°:2.3° for foot clearance during early swing.

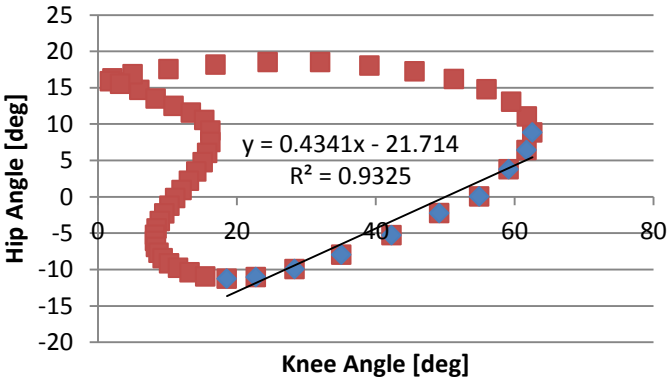

Figure 2. Hip - knee angles for slow able-bodied gait.

HKC design and testing

The first HKC hydraulic mechanism (**Figure 3a**) was designed, fabricated, and incorporated into the right upright of the HNP1 to coordinate flexion of the hip and knee joints during swing phase, where hip flexion

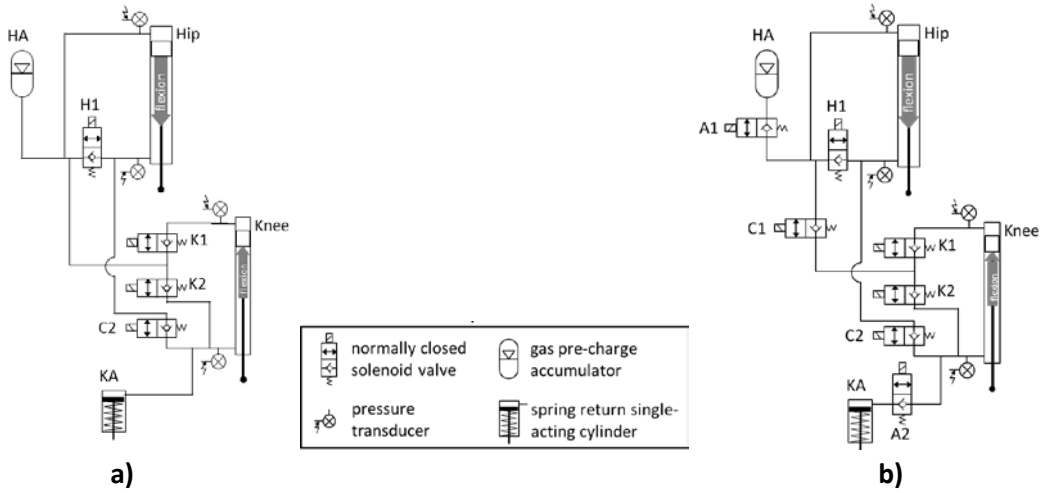

Figure 3. HKC hydraulic circuits for the right side, a) version #1 and b) version #2.

aided knee flexion. The hydraulic circuit had the states of hip independently freed or locked, knee independently freed or locked, and hip-knee coupled. The HNP1, with variable constraint hip mechanism (VCHM) and dual state knee mechanism (DSKM), was modified to incorporate a hydraulic HKC mechanism. Hip and knee hydraulic cylinders with the volume ratio of the two cylinders' rod sides were selected to achieve the approximate 1°:2.3° hip-knee ratio, according to the following equation:

$$\frac{volume_{hip}}{volume_{knee}} = \frac{\pi * \left(\frac{bore^2}{4}\right) * stroke}{\pi * \left(\frac{bore^2}{4}\right) * stroke} \approx 2.3$$

Components used in this unilateral HKC hydraulic circuit are listed in **Table 1**. The theoretical hip-knee ratio of the 7/8" bore hip cylinder and 9/16" bore knee cylinder was 1:2.4.

Table 1. Hydraulic Components for the HKC Mechanism

	Hip cylinder	Knee cylinder	Valve	Hip accumulator	Knee accumulator
Manufacturer	Clippard Minimatic	Clippard Minimatic	Allenair	Hydac	Clippard Minimatic
type	double acting	double acting	solenoid 2/2	gas pre-charge (58 psi) diaphragm	single acting spring return
bore	7/8”	9/16”	-	-	3/4”
port	1/16” NPT	1/16” NPT	1/8” NPT		1/8” NPT
orifice	-	-	2.38 mm	-	-
stroke	3”	3”	-	-	1”
rod diameter	0.25”	0.25”	-	-	0.25”
Size	-	-	-	0.075 L	
voltage	-	-	12 VDC	-	-
power consumption	-	-	7 W	-	-
C_V	-	-	0.176 B → A 0.166 A → B	-	-
response time (no load)	-	-	12 ms (on) 43 ms (off)	-	-
max operating pressure	2000 psi	2000 psi	-	3600 psi	250 psi
spring force	-	-	-	-	3 lbs installed 6 lbs compressed
cracking pressure	-	-	46 ± 7 psi	-	-

The bench-tested first version of the HKC hydraulic circuit (**Figure 3a**) did not function as expected. The hip-knee coupling ratio was inconsistent, i.e. movement of the hip cylinder did not always result in proportional movement of the knee cylinder since the fluid had access to the knee and hip accumulators. To improve upon this design, C1, A1, and, A2 valves (**Figure 3b**) were added in the HKC mechanism version #2 to block the flow to both accumulators and prevent fluid flow to the knee when the joints were moving independently.

Version #2 of the HKC hydraulic mechanism (**Figure 3b**) was used for bench testing to determine: (1) passive resistance due to the fluid in the hydraulic circuit, and (2) hip-knee joint coupling ratio of the mechanism. The hydraulic circuit was pressurized to approximately 70 psi to minimize compliance due to any remaining air bubbles in the circuitry. The hydraulic HKC mechanism was attached to the right upright of the exoskeleton of the HNP1 and affixed to a Biodex robotic dynamometer (Biodex Medical Systems Inc., Shirley, NY, USA) arm as shown in **Figure 4**. The dynamometer arm was set in passive mode and passive resistance (torque) was

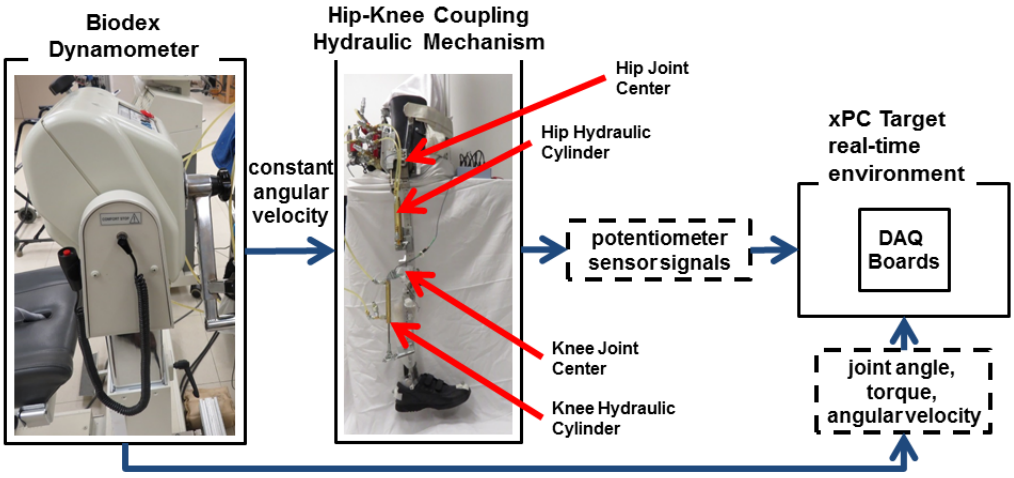

Figure 4. Diagram of bench test for HKC mechanism with Biodex dynamometer.

measured at constant angular velocities from 30 °/sec to 180 °/sec in 30 °/sec increments. Linear and rotary potentiometers (Vishay Spectrol, Malvern, PA, USA) measured the hip and knee joint angles, respectively. All dynamometer and potentiometer signals were sampled at 200 Hz and filtered online with a 5th order low-pass digital Butterworth filter with a cutoff frequency of 10 Hz. The pressure data were filtered online with a 7th order low-pass digital Butterworth filter with a cutoff frequency of 20 Hz. The dynamometer and angle data were filtered again offline with a 5th order low-pass digital Butterworth filter with a cutoff frequency of 3 Hz and 40 Hz, respectively.

HKC bench test results

Passive resistance – The torque resisting the movement of a joint at a specific angular velocity in the absence of any other actuation (muscle or motor) defines passive resistance. The average passive resistance at the hip measured at 30° of flexion when the joint was flexing (positive) and extending (negative) when the hip joint was moving independently at increasing angular velocities is shown in **Figure 5a** and when the hip and knee were coupled is shown in **Figure 5b**. Able-bodied gait kinematics show that the maximum angular velocity during gait occurs near a knee flexion angle of 30°.

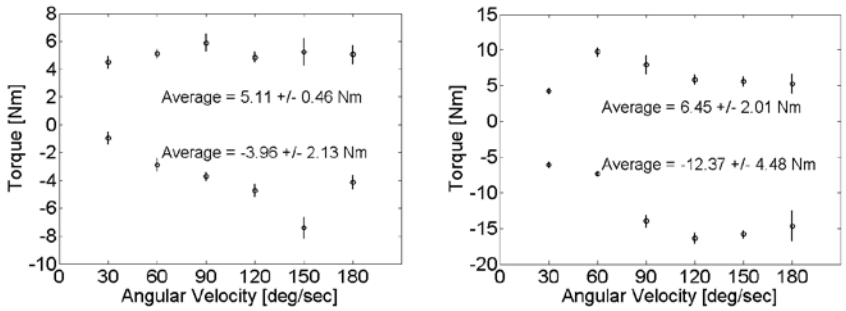

a) **b)**

Figure 5. Passive resistance of the hip at 30° of flexion when **a)** the hip was independently flexing (positive) and extending (negative) and **b)** when the hip was flexing and extending with HKC enabled.

Because passive resistance is a function of angular velocity, the largest amount of passive resistance is therefore expected at the knee angle of 30°. The passive resistance of the HKC mechanism generally increased with of angular velocity up to 90°/sec and then leveled off at 5.9 ± 0.6 Nm when the hip was independently moving in flexion. The increase in passive resistance was greater when the hip and knee were coupled and leveled off at an average of 7.9 ± 1.3 Nm when flexing and 13.7 ± 0.9 Nm when extending at an angular velocity of 90 °/sec.

Coupling ratios - Ratios between the hip and knee joint angles were determined as a function of angular velocity of the hip by averaging the slopes of the hip-knee plot at each joint (**Table 2**). The HKC ratio increased in flexion with an increase in angular velocity and remained essentially the same when the hip was extending.

Table 2. The average HKC ratio as a function of angular velocity

Angular Velocity	30 °/sec	60 °/sec	90 °/sec	120 °/sec	150 °/sec	180 °/sec
HKC ratio In Flexion	1.03 ± 0.48	1.14 ± 0.23	1.22 ± 0.28	1.28 ± 0.21	1.41 ± 0.18	1.52 ± 0.17
HKC ratio In Extension	1.08 ± 4.62	1.08 ± 0.35	1.07 ± 0.41	1.11 ± 0.45	0.85 ± 0.24	1.07 ± 0.33

Coupling delay and angle offset - During coupling of the hip and knee, there was a time delay between the start of hip flexion and the beginning of knee flexion. This delay was 136ms at 60°/s and decreased significantly to 9ms at angular velocity of 180°/s. In addition, there was an increase in offset of knee angle with respect to hip angle during cyclic flexion with continuous coupling as the angular velocity increased. This is attributed to compliance in the system due to residual air in the hydraulic circuit.

Summary of HKC mechanism bench testing

The passive resistance of the HKC increased when the hip and knee joints were coupled compared to movement of the joints independently. Approximately 13% of the hip flexion torque generated by NES (Kobetic 1994) would be needed to overcome the passive resistance observed during coupling, which would be metabolically and functionally inefficient.

Normative able-bodied data during gait show an approximate 1:2 ratio between the hip and knee joint angles in flexion while theoretical ratio based on cylinder volumes should be about 1:2.4. The prototype HKC mechanism exhibited an average hip-knee coupling ratio ranging between 1:1 and 1:1.5 during flexion, which increased slightly with increasing angular velocity. The variance in hip-knee coupling ratios may be due to compliance in the system from various sources. There was mechanical compliance in the rack and pinion gear used at the hip joint as well as from residual air trapped in the hydraulic system. The valves used in the hydraulic circuit can also be a potential cause for the inconsistent ratio between the hip and knee joint angles. Because the cracking pressure for the valves (eg. H1 or K2) is relatively low (46±7psi), fluid it may be that fluid was able to flow through them during operation, further contributing to variability in the coupling ration measurements.

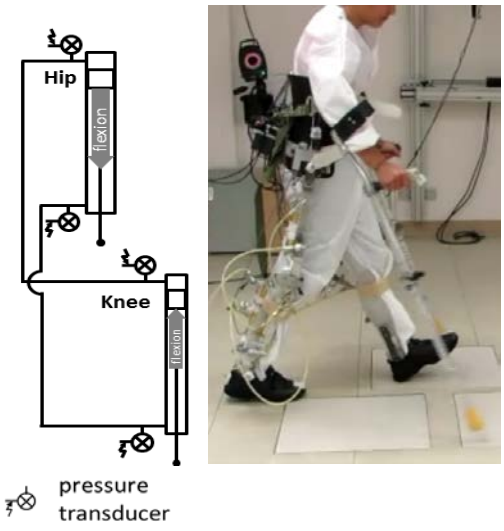

a) **b)**

Figure 6. a) HKC hydraulic circuit and **b**) able-bodied subject walking with HKC mechanism.

The time delay does not hinder the ability of the mechanism to create coupling between the hip and knee joint, but it does influence the resulting ratio between the hip and knee joints. Initiating hip flexion does not necessarily start knee flexion immediately. After a short time delay, the knee will begin to flex as a result of flexion of the hip. Implementing the HKC mechanism during walking may require planning for this time delay to ensure that sufficient knee flexion angle occurs to clear the foot during early swing.

The results show that hip-knee coupling with a hydraulic mechanism is feasible. However, there is a significant variability in coupling ratio, knee flexion delay and passive resistance which limits its practical implementation, as observed in our **separately funded** human testing with able-bodied (**Figure 6b**) and SCI subjects.

HKC mechanism implementation during walking with HNP1

A simplified version of the HKC hydraulic mechanism (**Figure 6a**) was incorporated into the HNP1 hardware to coordinate flexion of the hip and knee joints during swing phase of gait. The hip and knee hydraulic cylinders were of 7/8" and 9/16" bore, respectively, to achieve approximate HKC ratio of 1:2. The connections were between rod side of the hip cylinder and rod side of the knee cylinder (as well as blind side of the hip cylinder and blind side of the knee cylinder). The system was pressurized to approximately 60 psi to minimize compliance due to entrapped air.

The exoskeleton with bilateral HKC mechanism engaged was evaluated by an able-bodied volunteer (**Figure 6b**) and a subject with paraplegia from SCI (**Figure 8**). Both consented to participate in evaluation under a **separately funded study approved by the Investigational Review Board (IRB) at the Louis Stokes Cleveland VA Medical Center**. VICON motion analysis system, pressure sensor and potentiometer angle data from hip and knee joints were collected and post-processed to determine hip-knee coupling ratios.

Able-bodied evaluation of HKC – The ratio between the hip and knee (**Figure 7**) during the first half of swing phase was 1°:0.71±0.02° and 1°:1.84±0.11° during the second half of swing. An approximately linear relationship was found between joint angles during swing, however, there was no change in knee angle with significant change in hip angle during stance. The hip and knee joints showed some level of coupling as they both flexed (and extended) during swing phase. As previously mentioned, the inconsistent hip-knee coupling may have been due to poor mechanical coupling between segments at the exoskeletal joints (i.e. rack and pinion), compliance in the hydraulics due to

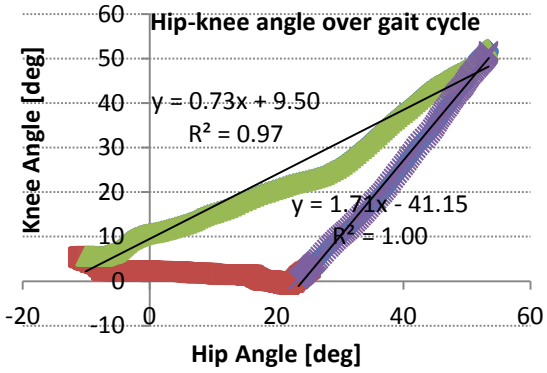

Figure 7. Linear fit to swing phase of hip-knee angle (first half of swing - green, second half-purple, and stance phase –red).

entrapped air and compliance in body-brace coupling. As a result, the HKC ratio exhibited during early swing phase was not as expected. It is unclear whether the subject took advantage of system compliance and used compensatory strategies in order to clear the foot, or volitionally assisted knee flexion.

Figure 8. Representative stride of hip-knee coupling condition, starting at left heel strike and ending at left heel strike.

SCI evaluation of HKC – The SCI subject initiated steps by pressing a finger switch to activate a pre-programmed pattern of stimulation delivered via percutaneous intramuscular electrodes to generate cyclic walking movements at a self selected speed with standby assistance for safety (**Figure 8**). Approximate hip-knee angle ratios were determined by from the ensemble averages of hip-knee angle data. With the HKC engaged, there was an approximate 1:1.2 ratio between the hip and knee angle (1° of hip flexion was 1.2° of knee flexion, R^2=0.97), compared to a ration of approximately 1:1.4 (R^2=0.18) with the hip and knee free to move independently. While some coupling occurred, it did not meet the expected ratio between the two joints as governed by the cylinder sizes. Thus, the subject was unable to achieve consistent foot-floor clearance. The HKC did not improve foot-floor clearance when compared to independent joint motion. With HKC mechanism engaged, the hip was flexed at the end of swing preventing the knee from fully extending. Therefore, the hydraulic circuit needs to be able to lock and unlock or decouple the hip and knee joints to allow the knee to extend and to prevent knee buckling during stance as muscles fatigue.

HKC incorporated into the HNP2

In an effort to reduce passive resistance, the hydraulic HKC mechanism was redesigned. New realizations of the VCHM and DSKM with fewer valves were incorporated into the new exoskeletal structure of HNP2 (***Task 2***) to eliminate rack and pinion compliance and other problems encountered in testing the HKC mechanism with HNP1. The prototype HNP2 exoskeleton provided independent hip locking/unlocking, knee locking and unlocking, hip-hip reciprocal coupling, or hip-knee coupling (**Figure 9**).

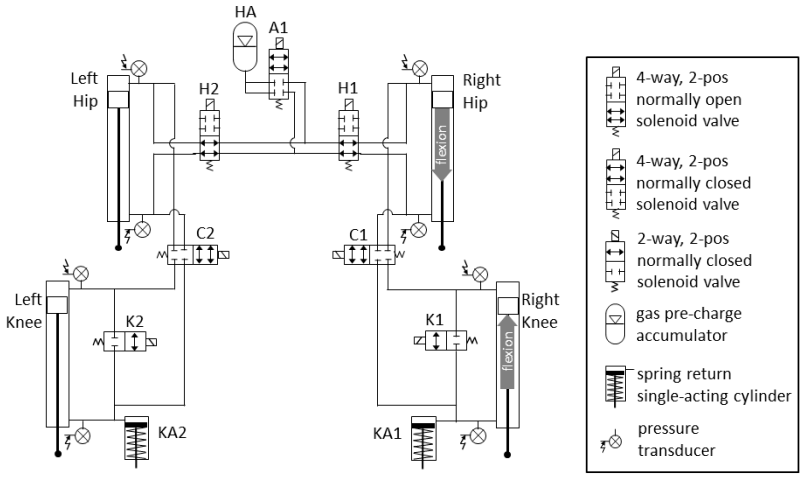

Figure 9. Hip-knee coupling bilateral hydraulic circuit.

Passive resistance of redesigned HKC – The inertial component of the torque needed to move the mass of the dynamometer arm and HKC mechanism was subtracted from the total measured torque to determine the resistive torque due to fluid flow in the hydraulic circuit. The hydraulic mechanism was attached to the right upright of the exoskeleton of the HNP2 mounted on an 8020 aluminum stand and affixed to the Biodex robotic dynamometer. The appropriate valves were activated to allow for either free movement of the hip while keeping the knee in a fully extended locked position or with hip and knee coupled. The dynamometer measured hip joint angle, angular velocity and torque. Hip joint angle was also recorded using rotary encoder (US Digital, Vancouver WA). Passive resistance was measured at constant angular velocities from 30 to 120°/sec in 30°/sec increments. One calibration trial was performed to measure the passive resistance due to the weight and inertial component of the upright and cylinders without functioning hydraulics at 30°/s. All dynamometer data were sampled at 200 Hz and filtered online with a 5th

order low-pass digital Butterworth filter with a cutoff frequency of 10 Hz. Offline processing included reapplying the same filter with a low-pass cutoff frequency of 3 Hz.

Passive resistance to independent hip movement – Hip passive resistance was measured with the knee locked in extension. The average passive resistance at 30° of flexion when the hip joint was independently flexing (negative) and extending (positive) at increasing angular velocities is shown in **Figure 10a** and as a function of hip angle in **Figure 10b**. The passive resistance generally increased as a function of angular velocity and does not appear to level off. As a function of hip angle, passive resistance at 60°/sec peaked at around 40-50° of hip flexion. A significant reduction in passive resistance was measured when valves were removed from the HKC hydraulic circuit and further when the length of tubing was minimized. Thus, a significant passive resistance was introduced by valves and tubing. Since these components are an integral part of the hydraulic circuit necessary for HKC control they cannot be eliminated.

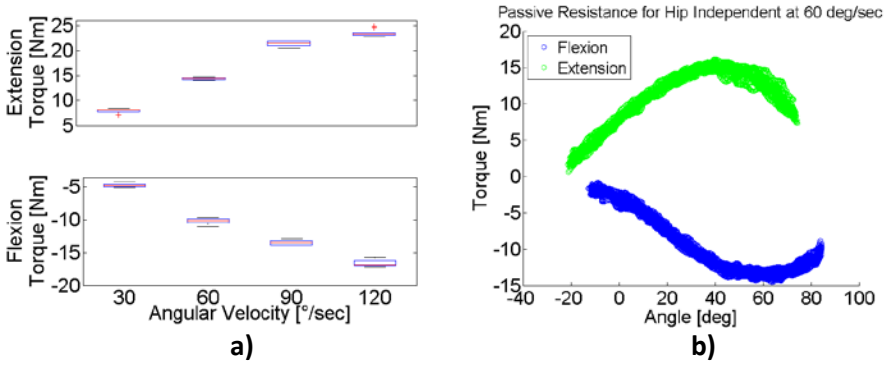

Figure 10. **a)** Passive resistance at 30° of hip flexion as a function of angular velocity and **b)** as a function of hip angle at 60°/s.

Passive resistance with hip-knee coupled – This experimental setup was similar to that used for the hip independent movement. To create hip-knee coupling function, valves H1 and C1 (**Figure 9**) were energized. The passive resistance increased with increased angular velocity (**Figure 11a**) and peaked at about 45° of hip flexion (**Figure 11b**). With the hydraulic hip-knee coupling, there was high passive resistance even when the valves were removed. Even though the hip-knee coupling ratios (between 1:0.96 and 1:1.00) with the newly fabricated uprights (HNP2) were more consistent, the passive resistance with hip-knee coupling makes this system impractical for use with available NES-generated hip flexion in individuals with SCI.

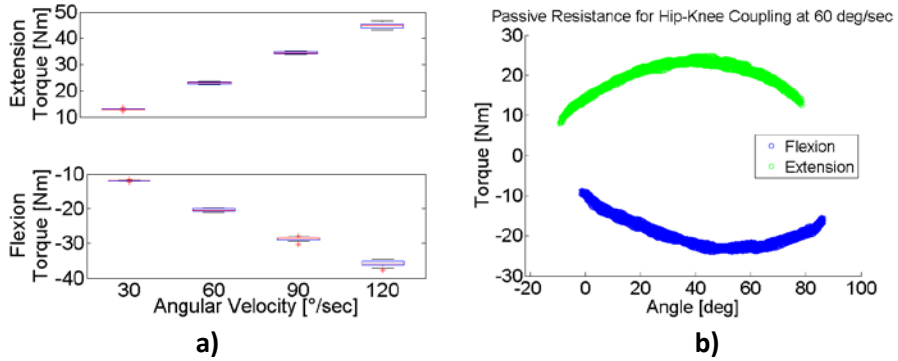

Figure 11. **a)** Passive resistance at 30° of hip flexion as a function of angular velocity and **b)** as a function of hip angle at 60°/s.

As an alternative to hydraulic hip-knee coupling to provide sufficient knee flexion for toe clearance during swing we pursued a mechanical solution consisting of instrumenting the knee joint with a spring loaded in extension. When released the flexion-biased spring causes knee and hip flexion at ratios dependent on the inertial properties of the leg and thigh segments, respectively[1]. The knee is extended to reload the spring in mid-swing by activating the quadriceps, thus requiring relatively small portion of the available knee extensor strength at a low duty cycle.

An elastomer spring ("The Knee Extension Assist," Fillauer Inc, Chatenooga TN) was mounted bilaterally at the knee to assist with knee flexion during pre-swing phase of gait. Bench testing determined that the elastomer was able to provide an estimated 11Nm of torque to flex the knee joint to 40° within 0.30±0.03s. When implemented in stimulation-driven SCI gait with the exoskeleton, the elastomer spring enabled the knee to reach peak swing phase flexion values of 45.1° ± 3.1° on the left and 43.7° ± 3.0° on the right. The right knee flexion showed a significant increase ($p<0.01$) in

[1] Huq MS, Tokhi OM, Genetic algorithms based approach for designing spring brake orthosis – Part I: Spring parameters. *Applied Bionics and Biomechanics*, 9:303-316, 2012.

knee flexion as compared to walking in the exoskeleton without the elastomer. The time to achieve 40° of knee flexion with the elastomer during SCI walking was on average 0.42 ± 0.05s, which is longer than determined in bench testing due to added limb inertia.

An alternative solution to improve knee flexion that can be explored in the future involves implantation of sartorius and gracilis muscles to provide hip and knee flexion with NES[2] alone or in a combination with a spring loaded mechanism.

Task 2 – Refine the design of the currently existing hybrid neuroprosthesis (HNP1) prototype orthosis and hydraulic system to minimize size, weight, enable rapid fitting, and provide easy donning and doffing in the field.

The uprights of the exoskeleton were redesigned to minimize weight, enable adjustability for fitting, make it easy for donning and doffing and provide for mounting of redesigned hydraulic mechanisms.

Exoskeleton Specifications

Structural dimensions - The design requirements for the HNP2 were specified for users with weight limit of 100 kg and stature between 5th percentile female and the 95th percentile male based on data from the National Health and Nutrition Examination Survey (NHANES). The representative measurements of the exoskeletal frame are included in **Table 3**.

Table 3. Structural dimensions

Measurement	Exoskeletal part	5th percentile female (cm)	95th percentile male (cm)
Floor to lateral femoral epicondyle	Leg upright with AFO	42	55
Lateral femoral epicondyle to greater trochanter	Thigh upright	36	47
Hip breadth	Corset/thoracic jacket bracket	29	36

Knee joint torque requirements - The maximum resistive torques required for most activities of daily living based on a 100 kg (220 lb) user were estimated and used to set design criteria for the new exoskeletal structure. The specifications were based on evaluation of HNP1 with MR damper controlling the knee combined with quadriceps stimulation during gait, the maximum damper torque utilized was 47 Nm, with a 63 kg user (Bulea 2012). Linearly scaling up for a 100 kg user yields a torque requirement of approximately 70 Nm. This is well above the specified torques for data published on exoskeletons reporting 0.35 Nm/kg and assumes some upper extremity support.

Hip joint torque requirements and specifications - The hip joint moments provide support and power assist functions**.** Hip joints for the HNP1 were designed to lock against an applied torque of 35 Nm during stance. However, during evaluation with SCI subjects the actual joint torques were less than 15 Nm (To 2010). To minimize the need for upper extremity support, the able-bodied locking torque of 0.4 Nm/kg (Winter 1991) or 40 Nm for a 100kg subject was used for this specification.

Actuators and Transmission Options

Rotary actuators - Adding hip-knee coupling capabilities to the HNP2 required either an equal exchange of fluid volume between hip and knee actuators, or inclusion of additional accumulators. A rotary actuator with equal fluid displacement on both sides of the sealed surface would eliminate the need for accumulators and the additional weight

[2] Kobetic R, Marsolais EB, Miller PC. Function and strength of electrically stimulated hip flexor muscles in paraplegia. *IEEE Trans Rehab Eng,* 2(1):11-17, 1994.

and complexity that they would add to the system. Furthermore, because the rotary actuators naturally produce rotary motion, the need for a transmission would be eliminated. For these reasons, a rotary actuator was designed, prototyped and bench tested for possible use in HNP2. This work was described in our annual report (*June 2014 Annual Report*). In summary, the actuator consisted of a 6061-T6 aluminum case and vane, utilizing rubber seals riding grooves cut in the vane to positively seal against leaking hydraulic fluid. Evaluation and testing revealed that the seal design needed further work, resulting in a maximum 100% sealing pressure of only 20 psi, and a rather high passive resistance of 12 Nm. Both of these deficiencies would require a major effort in redesign and fabrication beyond the scope of this study. Commercially hydraulic rotary actuators were also considered, but were found to be significantly heavier compared to traditional linear cylinders with rack-and-pinion joints. The linear cylinder based design originally incorporated in HNP1 was therefore retained for HNP2.

Rack and pinion gear - This arrangement was incorporated at the hip joint in HNP1, with the rack attached to the cylinder, and the pinion attached to the joint for a linear to rotary transmission. It was tested to 70 Nm of applied torque. The advantages of this transmission arrangement was simple design, constant moment arm and torque profile throughout the range of motion. The disadvantages of the gear material yield strength, weight, mechanical compliance or backlash, and possible bending moments of the cylinder rod eliminated this arrangement from consideration for inclusion in HNP2.

3-bar linkage - This arrangement was incorporated at the knee joint in the HNP1 with a 9/16" bore cylinder. The advantages were simple design, easy fabrication, low weight (especially important at distal joints), low compliance and versatility of linkage arrangement to maximize torque in specific range of joint movement. The disadvantages include moment arm and torque profile are a function of joint angle, singularities and points of zero moment holding capability (as in HNP1 at 75° of knee flexion). However, because of the many advantages offered by this transmission it was incorporated in the exoskeleton of the HNP2.

Hydraulic circuitry options and evaluation

Assessment of Hydraulic Components

Hydraulic valves were evaluated in an effort to reduce the size and weight of hydraulic circuitry in HNP2. Eight individual poppet type 2 way, 2 position solenoid valves (Allenair) in both normally closed (NC) and normally open (NO) configurations were used to construct HNP1, including one in each DSKM, and six in the VCHM. To add ability for hip-knee coupling, 14 additional valves of the same type would have been needed.

Cartridge valves - An alternative to the poppet-type valves are cartridge valves, offer a number of advantages in spite of being larger. Industrial cartridge valves are available in more complex configurations than discrete poppet valves, meaning that a single solenoid can control three, four, or six individual ports. This allowed all the necessary states to create the HNP2 to be implemented with seven 4 way, 2 position cartridge valves, rather than 14 individual 2-2ay, 2 position poppet valves. Cartridge valves also come with O–ring seals and threaded shafts for use in specially designed hydraulic manifolds. While individual manifolds are available, the real advantage is the possibility of creating a single manifold to hold multiple valves, thus reducing the size and weight.

High speed valves - Another option we explored was the high speed solenoid valve connected between the ports of a cylinder to regulate flow and to provide a measure of damping at the knee, which would be useful for controlling knee flexion during loading response phase of gait, during stand-to-sit and stair descent. It was hypothesized that a high speed variable closing and opening of the valve would be low pass filtered by the inertia of the system resulting in smooth controlled displacement of the cylinder and output motion at the knee. We tested a commercially available high speed valve from Clean Air Power for this application as described in our 2014 annual report (*Appendix C, June 2014 Annual Report*). The results showed that as a damper, the valve could only operate at low operating frequencies (10 Hz), where the valve has enough time to close, but at that frequency, the output motion was unacceptably jittery for inclusion in the hydraulic circuit.

Prototype servo based proportional valve - In the absence of commercially available industrial valves that provide sufficient resolution, a prototype proportional valve was designed, prototyped, and tested as described in our 2014 annual report (*Appendix D, June 2014 Annual Report*). At 200 psi, the valve allowed 0.86gpm of fluid to pass in its closed configuration which was significantly higher than the specified flow (0.3 to 0.7gpm) for the knee mechanism. While this

remains a potentially attractive solution to the problem, given limited time and resources this option was beyond the scope of this research project.

Manifold options **-** Brass fitting were used to interconnect hydraulic valves in HNP1. For the HNP2, manifolds were explored as alternatives to connecting hydraulic valves with connectors and tubing in an effort to save space, reduce potential for leakage, reduce resistance to flow and to create a cleaner appearance. Potential manifold solutions and their advantages and disadvantages were presented in our June 2014 Annual Report but were not incorporated into the HNP2 prototype given the overall complexity of the hydraulic circuit and the lack of flexibility to make modifications.

Exoskeleton Design

The exoskeleton of the HNP2 was designed to include thigh and shank adjustable overlapping double uprights with 1" by ¼" interconnecting members and coplanar cylinders mounted between to fit users of specified range of statures. This structure reduced the bending moments on the upright and the cylinders and was easy to manufacture and adjust for fitting. The uprights had a lateral projection of 5.8 cm and swivel abduction hip joints for ease of donning and doffing (**Figure 12a**). Abduction joins rotated about a shoulder bolt held in place with a nylock nut. To ensure smooth rotation, all bearing surfaces rode on oil-lite bronze bushings. The uprights attached to the pelvic band, which served as a corset-mounting frame and allowed anterior-posterior adjustment for hip joint alignment by means of a dovetail.

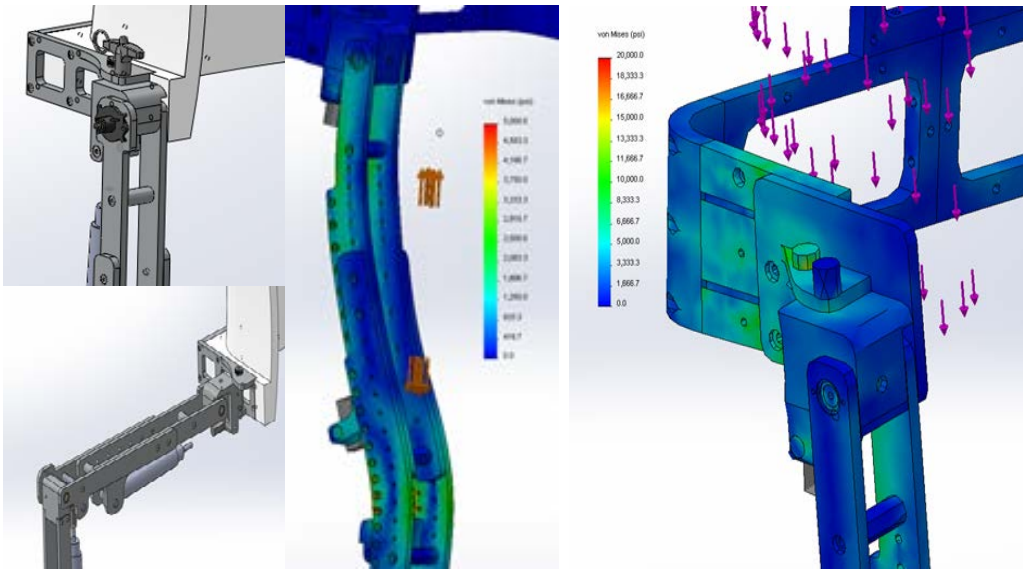

a) **b)** **c)**

Figure 12. SolidWorks drawing **a)** shows the uprights design with lockable swivel hip joint for easy donning and doffing while sitting in a chair. FEA of upright **b**) and pelvic frame with hip joint **c**) under loading conditions showing no significant stress concentrations that would compromise safety.

A Finite Element Analysis (FEA) was performed on the uprights and pelvic frame to assess the safety of the supporting structure, made from 6061-T6 Aluminum alloy, during loading. The upright was loaded with a maximum load of 330 kg applied at the cylinder attachment points as shown in **Figure 12b**. The maximum upright stresses were less than 5 ksi which meets > 2.5 safety factor against failure. Similarly, the pelvic frame was loaded with 90 kg while supported on a single upright. The stresses shown in **Figure 12c** produced by the loading were significantly lower than the yielding stress of 40 ksi for 6061-T6 Aluminum alloy, thus, structurally sound against failure.

The prototype exoskeleton (**Figure 13**) was manufactured, assembled and instrumented with encoders to measure hip and knee angles for feedback control. All movements were smooth and unhindered except for passive resistance of hydraulic mechanisms. Pin lock hip abduction joints provided a positive lock and engagement to prevent accidental release and can be removed for ease of donning/doffing with uprights abducted. A back plate attached to the pelvic frame provides mounting structure for the corset, hydraulic valves, batteries and electronics for signal processing and valve and stimulation control. Attachments for the custom fitted orthotic components (ankle foot

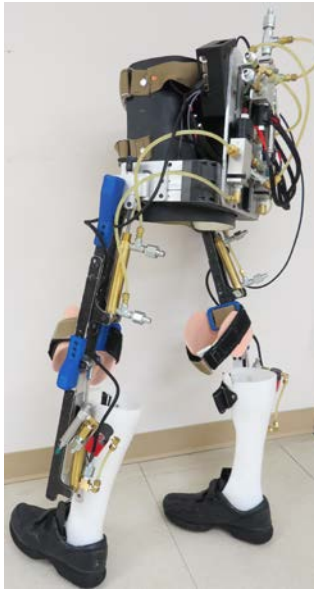

Figure 13. Assembled exoskeleton for HNP2.

orthoses (AFOs) and thoracic corset) to the exoskeleton were designed and implemented. The shank upright has attachment holes for fitting by adjusting AFO mounting. These custom fitted orthotic components allow for efficient motion transfer from the user to the exoskeleton and prevent potentially injurious high pressure concentrations on the skin. Attachments for Velcro thigh cuffs were designed, 3D printed, and provided a close coupling between the exoskeleton and the user.

Variable Constraint Hip Mechanism

To minimize the size and weight of the hydraulic circuit, the VCHM and DSKM of the HNP1 were redesigned and incorporated into the HNP2 to allow hip independently freed or locked, hip-hip reciprocally coupled, and knees independently free or locked. The two 2-way valves of the original VCHM were replaced with one 4-way, 2-position valve as shown in **Figure 14**. The 9/16" bore cylinder in the original DKSM was replaced with a 7/8" bore cylinder to meet stand-to-sit torque requirements. The assembled circuit was bench tested for passive resistance of the right hip independent motion, hip-hip reciprocal coupling motion, and right knee independent motion.

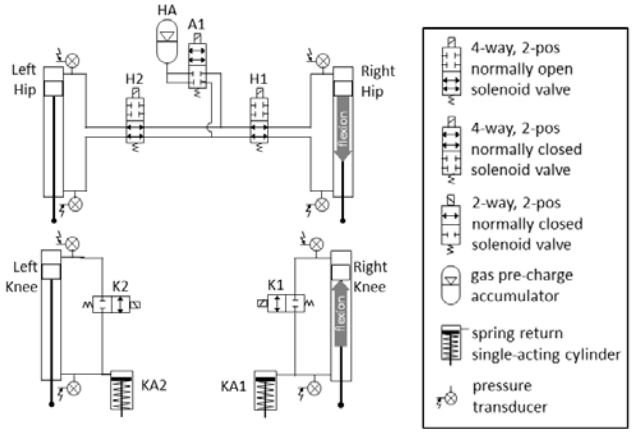

Figure 14. HNP2 hydraulic circuit schematic.

The hydraulic circuit schematic shown in **Figure 14** was assembled as shown in **Figure 15**, using the components listed in **Table 4,** for bench testing to (1) analyze the passive resistance due to the hydraulics and (2) determine the locking torque and compliance at the hip and knee joints. The system was pressurized (i.e. precharged) to approximately 70 psi to reduce the effect of entrapped air bubbles after priming.

Table 4. Hydraulic Components for VCHM and DSKM Mechanisms.

	Hip and knee cylinders	**Hip valves**		**Knee valve**	**Hip accumulator**	**Knee accumulator**
Manufacturer	Clippard Minimatic	Hydraforce	Hydraforce	Allenair	Hydac	Clippard Minimatic
type	double acting	4-way, 2-pos Normally Closed	4-way, 2-pos Normally Open	2-way, 2-pos Normally Closed	gas pre-charge (58 psi) diaphragm, 0.075 L	single acting spring return
bore	7/8"	-	-	-	-	3/4"
port	1/8" NPT	SAE 6	SAE 6	1/8" NPT	SAE 6	1/8" NPT
stroke	3"	-	-	-	-	1"
rod diameter	0.25"	-	-	-	-	0.25"
voltage	-	12 VDC	12 VDC	12 VDC	-	-
power consumption	-	14.4 W	14.4 W	7 W	-	-
max operating pressure	2000 psi	3000 psi	3000 psi	46 ± 7 psi (cracking pressure)	3600 psi	250 psi
spring force	-	-	-	-	-	3 lbs installed 6 lbs compressed

Figure 15. VCHM2 and DSKM2 hydraulic circuit realizations with electronics attached.

The hydraulic mechanism was attached to the upright of the exoskeleton of the HNP2 and affixed to the Biodex® dynamometer arm (**Figure 16**). Valves A1 and H2 were energized to test hip independent function, no valves were energized to test default hip reciprocal coupling and valve H1 was energized to lock the right hip. For the knee test, valve K1 was energized to free the knee for passive resistance test and de-energized to lock the knee to measure locking torque and compliance. Hip and knee joint angles were recorded using rotary encoders (US Digital, Vancouver, WA, USA) during dynamometer arm movements through the range of motion. The dynamometer set in passive mode measured the joint angle, angular velocity, and torque due to passive resistance at constant angular velocities from 30 to 120°/s in 30°/s increments. Calibration measuring the passive resistance due to the weight and inertial component of the upright and cylinders without functioning hydraulics at 30°/s was subtracted from the total torque to determine the passive resistance due to the hydraulic system. Dynamometer data were collected at 200 Hz and filtered online with a 5th –order low-pass digital Butterworth filter with a cutoff frequency of 10 Hz and again offline with a low-pass cutoff frequency of 3 Hz. The encoder data were filtered offline with a moving average filter (50 ms).

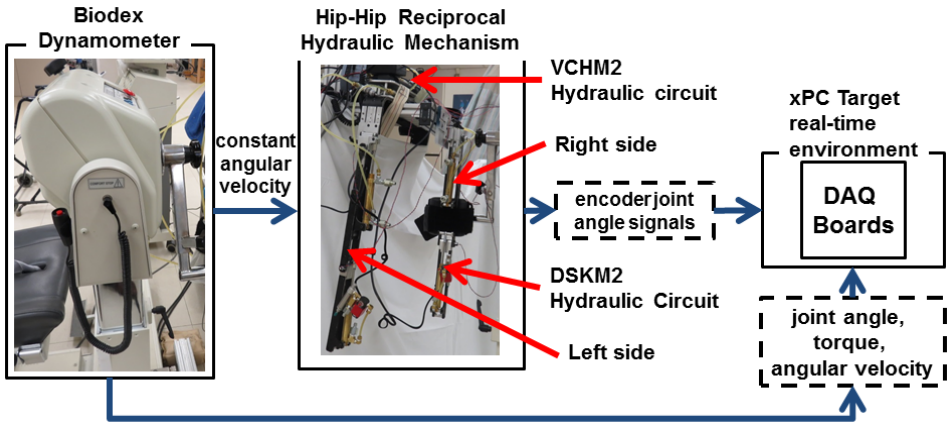

Figure 16 . Experimental setup with Biodex dynamometer.

Hip passive resistance – The average passive resistance at 30° of flexion when the hip joint was flexing (negative) and extending (positive) at increasing angular velocities is shown in **Figure 17**. In general, the passive resistance increased linearly with angular velocity, as well as a function of hip angle at a constant angular velocity. For example, at 60°/s the passive resistance increased up to 45° of hip flexion to a peak torque of 12 and 17 Nm for hip independent and hip-hip reciprocally coupled movements, respectively.

Hip locking torque and compliance - The VCHM2 was specified to resist at least 40 Nm of applied torque[3] to support a subject with SCI during walking. Dynamometer was used to manually apply a flexion torque about the locked hip joint with compliance defined as a change in angle with applied torque.

The VCHM2, with hip cylinder locked, was able to withstand at least 60 Nm of applied flexion torque, exceeding the needed support moment against hip flexion for a person with paraplegia. The compliance increased with applied torque to approximately 8° at 35 Nm, to an approximate maximum of 10-12° at 60 Nm.

Hip reciprocal coupling ratio – In its default state the VCHM2 has the function of coordinating the right hip with the left hip i.e. for every degree of right hip flexion there should be an equal left hip extension. The relationship between the right and left hip angles during early swing was determined using the rotary encoders, namely the hip-hip reciprocal coupling ratio. This coupling ratio remained within 3 to 4% of the 1:1 design criteria for all angular velocities tested up to 120°/s.

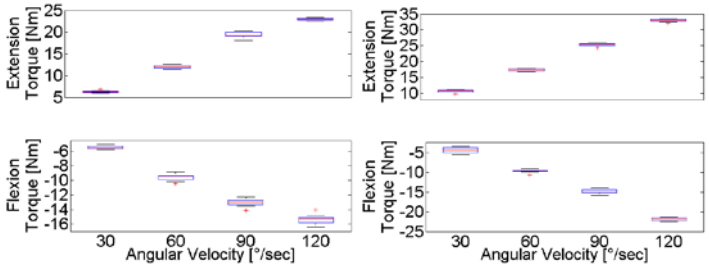

Figure 17. Passive resistance at 30° of flexion for the VCHM2 when the hip is flexing (negative) and extending (positive) for **a)** hip independent and **b)** L hip-R hip reciprocally coupled.

Dual State Knee Mechanism

Knee passive resistance – The inertial component of the torque measured on the dynamometer was subtracted from the total torque. The average passive resistance measured at 30° of knee flexion and extension increased with increasing angular velocity to approximately 4 Nm at 120°/s. Similarly, the passive resistance increased as a function of knee angle when moving at constant angular velocity. The passive resistance of the knee mechanism at an angular velocity of 60°/s also increased with flexion and leveled off at 3 Nm.

Knee locking torque and compliance - The DSKM2 was specified to resist at least 70 Nm of applied torque at or near full knee extension, which should be able to support a subject with SCI during stance phase of gait. Knee flexion torque up to 70 Nm was applied with robotic dynamometer on a locked mechanism in each trial (**Figure 18**). Compliance, the change in angle, increased with applied torque. The DSKM2 was able to withstand at least 70 Nm of applied flexion torque at approximate compliance of 4°, thus meeting specifications.

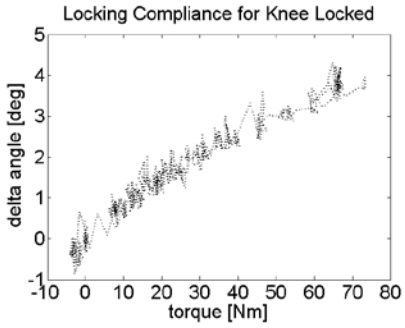

Figure 18. Compliance of the locked DSKM2 as a function of applied torque.

Summary of HNP2 Exoskeleton Structure and Hydraulic System

The HNP2 exoskeletal structure is lighter and more easily adjustable for fitting, donning and doffing than the earlier HNP1 prototype. The new redesigned hydraulic circuits provide comparable function with fewer components and decreased posterior projection. The self-contained HNP2 weighs 18.1kg, which is 18.5% lighter than the previous tethered HNP1 prototype.

However, the resulting hydraulic passive resistance for the VCHM2 is comparable to or slightly higher (7% of hip flexion torque and 10% of hip extension torque) than the VCHM1 with median torques up to but not exceeding 6 Nm[4]. NES is capable of generating about 60 Nm of hip flexion torque and 70 Nm of hip extension torque[5]. Thus, approximately 18% of the hip flexion torque and approximately 22% of the hip extension torque generated by NES in persons with SCI is required to overcome the passive resistance during hip independent motion. This effort would

[3] Perry J. Gait Analysis: Normal and Pathological Function. Thorofare, NJ: SLACK Incorporated, pp. 92, 94, 1992.

[4] To CS. Closed-loop control and variable constraint mechanisms of a hybrid neuroprosthesis to restore gait after spinal cord injury. PhD Dissertation, Case Western Reserve University, 2010.

[5] Kobetic R, Marsolais EB. Synthesis of paraplegic gait with multichannel functional neuromuscular stimulation. *IEEE Trans Rehab Eng.* 3(2): 66-79, 1994.

increase to 21% of the hip flexion torque and approximately 31% of the hip extension torque to overcome the passive resistance during reciprocal coupling of the hips. Primary cause for the increased passive resistance is likely the combination of tubing/hose length and new valves.

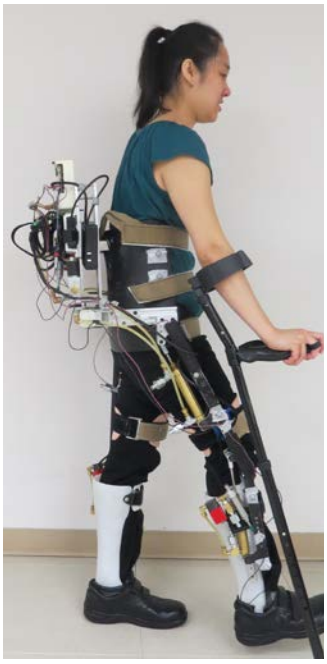

Figure 19. Able-bodied subject fitted with HNP2.

The locking torque for the hip mechanism was able to withstand at least 60Nm of applied flexion torque, thus meeting specification for providing sufficient moment to maintain posture. The compliance of the hip mechanism at the load of 35Nm is about 7-8° and increases to about 10-12° of flexion at 60Nm. This compliance is comparable to the amount of trunk tilt seen in reciprocating gait orthoses[6]. The VCHM2 and uprights allow for a few degrees of flexion when the hips are locked but still support the user from an excessive forward lean which is further prevented by the 1:1 hip-hip reciprocal coupling (i.e. one degree of right hip flexion will result in one degree of left hip extension). This constraint restricts the hips from simultaneously moving in the same direction to avoid the tendency for bilateral hip flexion and forward trunk lean.

The passive resistance of the DKSM2 knee joint was also higher than the previous design. About 17% of the knee flexion moment and 3% of the knee extension moment generated by NES is required to overcome the passive resistance in flexion and extension, respectively[7]. This increase in passive resistances is due to the larger 7/8" bore cylinder with larger stiction and viscous effects. Generating enough knee flexion for walking may be challenging with NES stimulation alone and an elastic knee assist has been explored to counter the added weight and passive resistance created by the DSKM2 with a larger cylinder. The DSKM2 was able to support up to 70Nm with a compliance of 4° of flexion. This is a negligible and acceptable compliance in the locked knee joint when loaded.

While it was easy for an able-bodied individual to walk with the HNP2 (**Figure 19**), as determined in a **separately funded study supported by the US Department of Veterans Affairs**, subjects with SCI may require assistance due to the passive resistance of the device and reduced stimulated joint torque output which can be further compromised by muscle fatigue. To obviate these limitations in future hybrid neuromechanical gait assist systems, small motors could be incorporated at hip and knee joints to provide the additional power as needed to maintain the speed and distance and overcome obstacles for community ambulation.

Task 3 – Design, develop and implement a new control system to automatically coordinate electrical stimulation with hydraulic exoskeleton using a mobile computing platform.

The aim of this task is to untether hybrid neuromechanical system and design and implement mobile computing platform for HNP2 for use outside of the laboratory. Supporting hardware and software was developed for control and data acquisition for evaluation of the HNP1 (**Figure 20**) as described in the Final Report Award Number: W81XWH-05-1-0389. Custom circuitry was developed and integrated with instrumentation and computers at the Motion Studies Laboratory at the Louis Stokes Cleveland VA Medical Center. This allowed for the xPC Target (The MathWorks, Inc., Natick, MA, USA) prototyping environment to execute Simulink models in real time for controlling the HNP1 system. The target PC provided sensor signal acquisition and the output of control states to the exoskeleton. All communication between the target PC and the exoskeleton was through a multi conductor cable at a frequency of 200 Hz during laboratory experiments. The host PC ran Matlab®/Simulink® and was responsible for building the target application into the target PC and controlling the target application during operation. The host and target computers communicated via the TCP/IP protocol. The host PC ran a graphical user interface (GUI) which was developed to simplify the building, calibration, implementation, and testing of the HNP controller. The GUI sent commands to and acquired signals from

[6] Marsolais EB, Kobetic R, Polando G, Ferguson K, Tashman S, Gaudio R, Nandurkar S, Lehneis HR. The Case Western Reserve University hybrid gait orthosis. *J Spinal Cord Med*., 23(2): 100-108, 2000.

[7] Kobetic R, Marsolais EB. Synthesis of paraplegic gait with multichannel functional neuromuscular stimulation. *IEEE Trans Rehab Eng.* 3(2): 66-79, 1994.

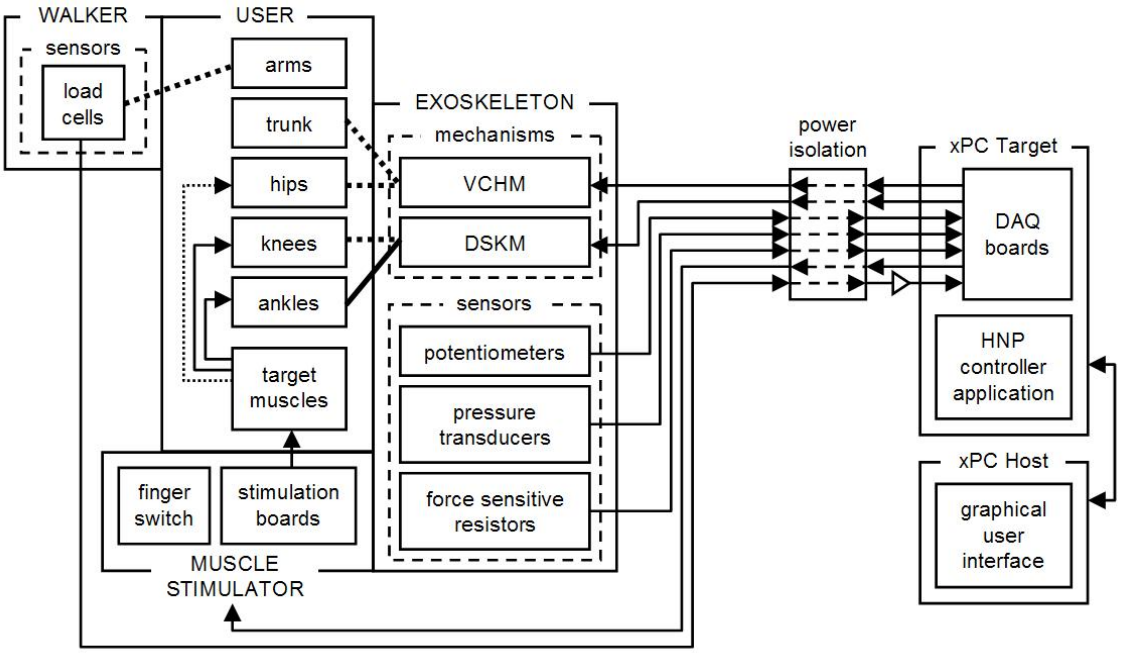

Figure 20. Hardware for controller of the HNP consists of xPC target computer, xPC host computer, and the muscle stimulator.

the target PC during real-time implementation. The muscle stimulator unit delivered the NES to target paralyzed muscles to drive limb motion. The activity states were selected through button polling and displayed on the liquid crystal display. Steps were initiated either by a push button, automatically cycled until stopped or initiated by a sensor. When STOP button was pressed during walking, the stimulation pattern transitioned into the standing stimulation pattern at the end of the step. A scroll button was programmed to provide subject options to walk, climb stairs or sit down.

The HNP1 control consisted of the finite state knee controller (FSKC) for the dual state knee mechanism, the finite state postural controller (FSPC) for the variable constraint hip mechanism and the NES controller.

HNP2 Hardware and Software Development

The HNP2 mobile control system hardware includes embedded control board, signal conditioning board, stimulation board, sensors, and power supply as shown schematically in **Figure 21**. The embedded control board (ECB) is the brain of the HNP2. It interfaces with the signal conditioning board and stimulation boards.

An Arduino-based embedded control system communicates with PC for controller development and downloading, with mobile devices (smart phones) for user interface, with neuromuscular electrical stimulation boards to send out stimulation commands and signal conditioning board.

Embedded control board (ECB) - Analog sensor signals are sampled by a custom embedded control board (**Figure 22**), which generates the digital valve control signals. The ECB can communicate with a PC/laptop either wirelessly or through a USB port for software development. In addition, ECB communicates wirelessly with an Android-based smart phone or a hand switch user interface for selecting and activating functional tasks (i.e. stand-up, sit down, walk, climb stairs, etc.).

The main control unit is the ATmega2560 processor. This is a high-performance, low-power Atmel 8-bit AVR RISC-based microcontroller which combines 256KB ISP flash memory, 8KB SRAM, 4KB EEPROM, 86 general purpose I/O lines, 32 general purpose working registers, real time counter, six flexible timer/counters with compare modes, PWM, 4 USARTs, byte oriented 2-wire serial interface, 16-channel 10-bit A/D converter, and a JTAG interface for on-chip debugging. This supports 16 channels of PWM digital output for hydraulic valve control or motors. The device achieves a throughput of 16 MIPS at 16 MHz and operates between 4.5-5.5 volts.

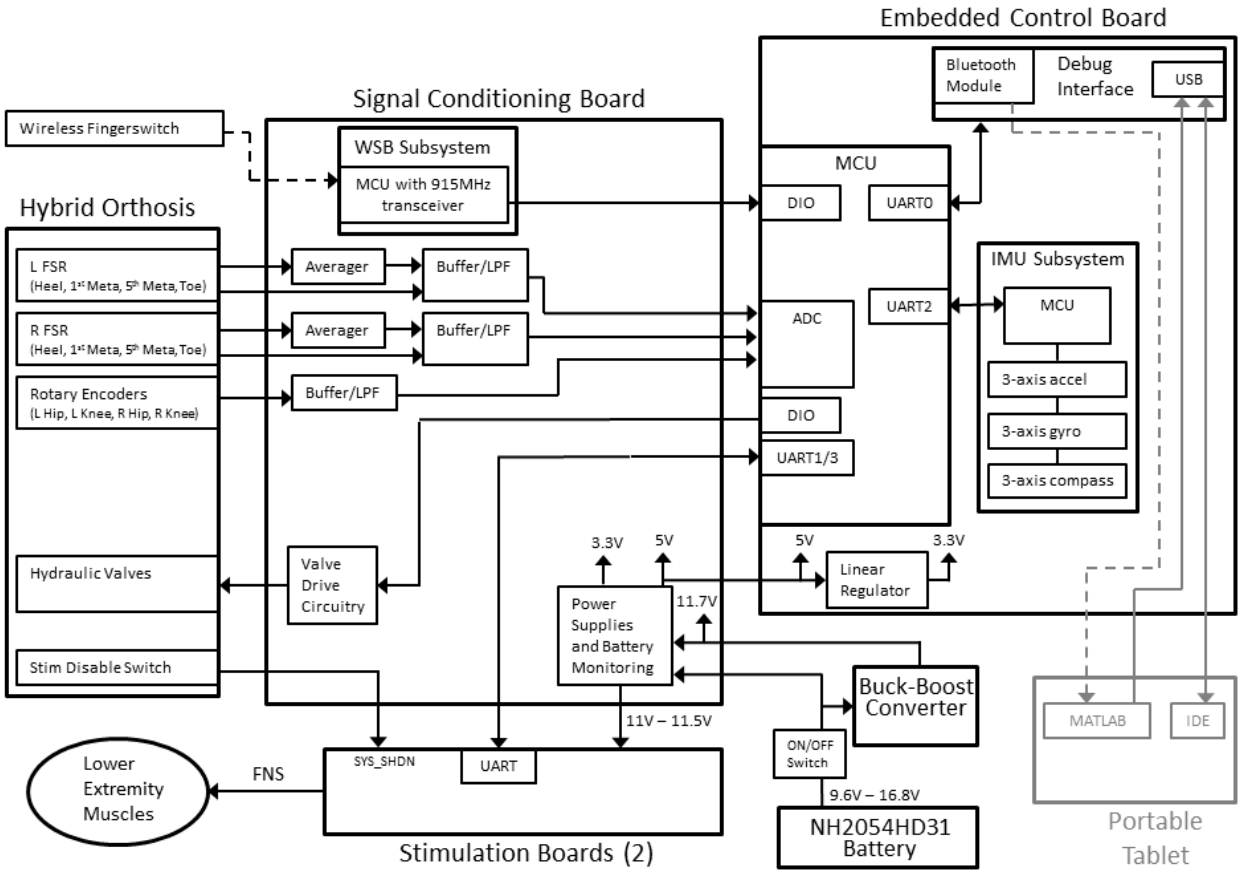

Figure 21. HNP2 control hardware block diagram.

An ATmega328 microcontroller is used as co-processor for data fusion and filtering and communicates with the main processor by UART port. The MPU-9150 nine axes inertial measurement unit (IMU) includes accelerometer, gyroscope and compass to provide capabilities to measure 3D linear accelerations, angular velocities and compass orientations.

The control unit communicates with stimulation boards through Universal Asynchronous Receiver/Transmitter ports (UART). There are two kinds of stimulation boards that can provide stimulation with either percutaneous intramuscular or surface electrodes. In addition, there is an implant communication board that sends command signals to an implanted receiver stimulator. All stimulation boards can be used either by themselves or in combination with others.

The ECB runs the finite state controller which, based on sensor inputs, user command, and an onboard inertial measurement unit (IMU), provides control signals to activate and deactivate the solenoid hydraulic valves to either lock or free the knee joints and lock, free or couple the hip joints. The ECB also sends control signals to the stimulation board for muscle activation and synchronizes it with activities of the exoskeletal joints based on gait event detector.

Signal conditioning board **(SCB)** - Sensor signals from left and right force sensing resistors (FSRs) placed between the AFOs and shoes, encoders at hips and knees, and hydraulic pressure sensors at the pistons are amplified, filtered and processed by a custom signal conditioning board. The SCB also provides control/drive signals for hydraulic valves and interface to stimulation board. It generates the necessary voltages (power supplies) for circuitry,

Figure 22. Controller hardware including Embedded Control Board (top left), Signal Conditioning Board (middle) and 2 stimulation output boards (bottom).

sensors, and valves. In addition, the SCB includes wireless sensor board subsystem to provide communication with wireless finger switch and any wireless accelerometers and gyroscopes mounted on the exoskeleton for feedback control.

The signal conditioning board, embedded control board and stimulation boards are stacked in the enclosure for ease of connections (**Figure 22**). The circuitry can be controlled remotely by a smart phone and stream data wirelessly to a PC/laptop.

The HNP2 system is powered by an Inspired Energy NH2054HD31 lithium ion battery pack (14.4V, 6.2 Ah, 436gm, 15.2cm x 7.9cm x 2.3cm). A regulated 11.7 V power supply is generated by a buck-boost converter.

NOTE: No human subject testing was supported by this project (contract W81XWH-13-1-0099), which only entailed the design and bench testing of the technical components of the untethered HNP2 prototype and new wireless communication and control system. Able-bodied and SCI testing of the resulting prototype devices were conducted under a separately funded project supported by the US Department of Veterans Affairs.

Able-bodied Testing of the Untethered HNP2

A graphical user interface (GUI) on PC/laptop communicates wirelessly with a finite state machine (FSM) controller running onboard HNP2. A gait event detector (GED) was validated in an able-bodied subject (**Figure 23a**) who consented to participate in evaluation under a protocol for hybrid neuroprosthesis evaluation approved by the Institutional Review Board at the Louis Stokes Cleveland VA Medical Center. The GED utilized foot-floor contact pressures as sensed by the FSRs as inputs to the finite state controller running on the ECB to couple the hips and free or lock the knees during swing and stance phases, respectively. For example, the subject indicated intent to make a step by shifting weight to the contralateral leg, thus unloading the ipsilateral FSRs causing the knee to unlock for swing. The same knee was then locked for stance at heel strike in preparation for next step while the process repeated for the other side. Sensor signals from the hip and knee joints and FSRs were streamed wirelessly to PC/laptop for real time display on a GUI and post-processing (**Figure 23b**).

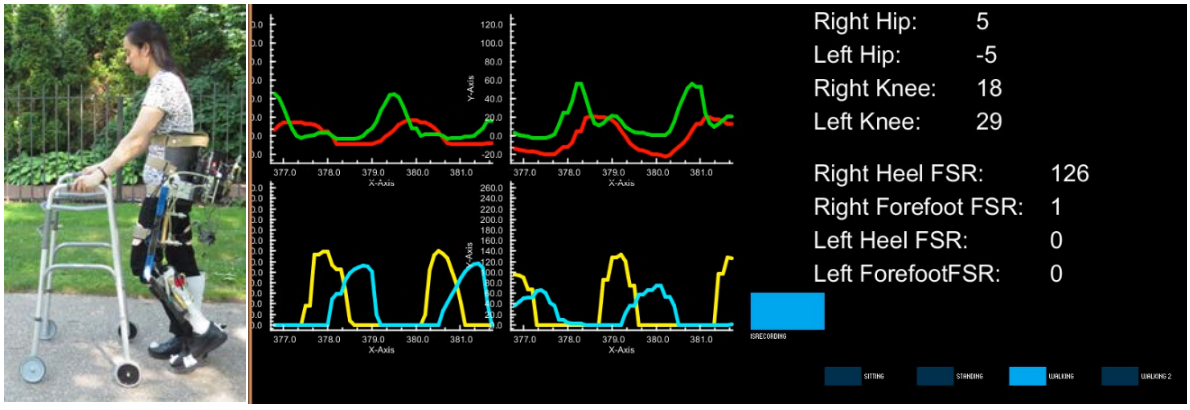

a) **b)**

Figure 23. a) Able-bodied subject walking with untethered HNP2, and **b)** wirelessly streamed real time hip and knee angle and FSR data from embedded control board displayed on a remote PC.

HNP2 Testing in Individuals with SCI

The untethered HNP2, a stimulation-driven exoskeleton, was used to restore stepping in individuals with motor complete paralysis due to spinal cord injury (SCI). Users interacted with the system via a custom wireless finger switch to indicate the intent to stand-up, step, or sit down. The transitions between states of the FSM for progression through the gait cycle were triggered from a combination of the sensor signals. These included joint encoders (US Digital, Vancouver, WA, USA) and force sensitive resistors (B & L Engineering, Tustin, CA, USA). Encoders were located

bilaterally at each of the hip and knee joints on the exoskeleton to measure joint angles. Insoles with the force sensing resistors (FSRs) under the 1st and 5th metatarsals, 1st phalange, and heel monitored foot-floor contact pressure.

The SCB conditioned and filtered the sensor signals and generated the drive signals for the hydraulic valves. The ECB interfaced with the SCB and stimulation boards by sampling the analog sensor signals and generating the digital valve control signals based on the rules of the finite state controller. The ECB also contained an inertial measurement unit and Bluetooth module. The ECB communicated with a computer wirelessly via the Bluetooth module, or through a wired USB port.

Assessment of the HNP2 was completed on three individuals with SCI who consented to participate in an evaluation protocol approved by the Institutional Review Board of the Louis Stokes Cleveland VA Medical Center and separately funded. The muscle set utilized varied for each subject and are listed in **Table 5**, along with other pertinent physical characteristics.

Common embedded controller and signal conditioning boards were used for all testing, while stimulation hardware was customized for each individual volunteer. Subject A had two 12-channel percutaneous intramuscular stimulation boards; Subject B used one communication board for a16-channel implanted stimulator transmitter (IST) and one 4-channel bipolar surface stimulation board; and Subject C had two implant communication boards: one for a16-channel IST and a second one for a8-channel implanted receiver stimulator (IRS). Stimulus pulse width was controlled on a pulse-by-pulse basis while current amplitude and frequency were set for each channel individually. Each percutaneous stimulation board was capable of providing up to 12 channels of stimulation at amplitudes up to 20mA and pulse widths up to 250µs, while the surface stimulation board was able to provide up to 4 bipolar channels or 7 monopolar channels of stimulation with amplitude of up to 100mA and pulse widths up to 250µs. Implant control modules could command the IRS or IST implanted pulse generators to deliver stimulus waveforms on individual channels of up to 20mA in amplitude and pulse widths up to 250µs, depending on whether an intramuscular or cuff electrode was used.

Table 5. Characteristics for participants

Subject	**A**	**B**	**C**
Sex	M	M	M
Age (yr)	54	56	59
Weight (kg)	64	92	79
Height (cm)	175	193	175
Injury Level	T4	T11	C7
AIS	AIS A	AIS B	AIS B
Time Since Injury (yr)	32 (11/27/83)	7 (1/29/09)	8 (3/9/08)
Time Since Implant (yr)	31 (6/1/84)	4 (5/2/11)	4 (1/16/12)
Stimulation Boards Used	Two percutaneous	One IST-16 and one bipolar surface	One IST-16 and one IRS-8
Muscles Stimulated	PA, GM, VM, VL, QD, TFL, ST, GR, TA	PA, GM, ME, HS, QD, WD	PA, GM, ME, HS, QD, TFL, ST, IL, TA

AIS: American Spinal Injury Association Impairment Scale, C: cervical, GM: gluteus maximus, GR: gracilis, HS: hamstrings, IL: iliopsoas, ME: gluteus medius, PA: posterior portion of adductor magnus, QD: quadriceps, ST: sartorius, T: thoracic, TA: tibialis anterior, TFL: tensor fasciae latae, VM: vastus medialis, VL: vastus lateralis, WD: widthdrawal reflex

Controller software - A finite state machine (FSM) was designed to coordinate stimulation patterns with the appropriate hydraulic joint constraints. Sensor signals (wireless finger switch button presses, joint encoders, FSRs) were used to transition into the correct state of the FSM. The high-level control of the FSM included *sitting*, *sit-to-stand*, *standing*, *stepping*, and *stand-to-sit* states and delivered the appropriate stimulation patterns specific to each participant (**Figure 24**). High-level transitions were user initiated by button presses on the wireless finger switch. The brace default and initial state was in the *sitting* state, with the hips reciprocally coupled, knees locked, and all stimulation turned off. The user could choose to unlock all joints to adjust the sitting position before transitioning from the *sit-to-stand* state initiated by pressing the "go" button. This uncoupled/unlocked the hips, unlocked the knees, and ramped up stimulation to the hip and knee extensor muscles. When in a good upright posture with all joints at neutral, the user pressed the "go" button to lock all joints (*standing* state) and simultaneously *calibrate* the joint angle encoders (re-zero joint angles). From standing, the user could choose to transition into the *stepping* state or to *stand-to-sit*. If the user desired to initiate the *stand-to-sit*, the "stop" button unlocked all joints and ramped down stimulation to the hip and knee extensor muscles for returning to the *sitting* state.

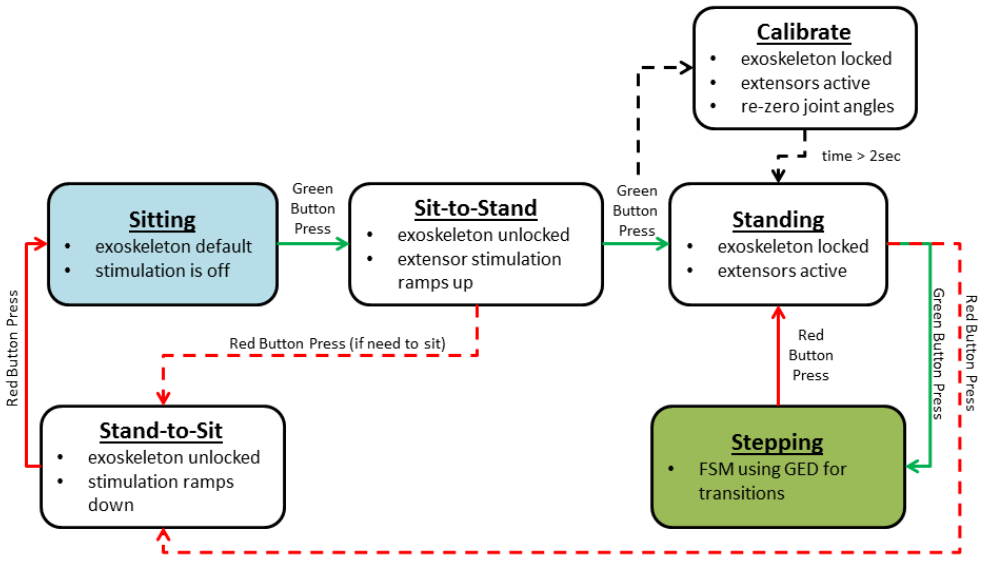

Figure 24. High-level control system

When entering the *stepping* state, the FSM used the gait event detector (GED) to alternate between left and right steps and switch between phases of gait to deliver the left or right step stimulation pattern while adjusting the hydraulic joint constraints appropriately[8]. The GED detected transitions between *double stance (to left swing)*, *left early swing*, *left late swing*, *left weight acceptance*, *double stance (to right swing)*, *right early swing*, *right late swing*, and *right weight acceptance* phases during stepping (**Figure 25**). Sensor thresholds for the GED were initially selected from nondisabled volunteer testing and heuristically adjusted as necessary for the SCI subjects. *Double stance*, *early swing*, *late swing*, and *weight acceptance* phases alternated between left and right sides. During *left early swing* phase, the right (contralateral) knee was locked and the left (ipsilateral) knee was unlocked. Similarly, during *right early swing* phase, the left (contralateral) knee was locked and the right (ipsilateral) knee was unlocked. *Double stance* phase was initiated when both ipsilateral and contralateral heels or forefeet were in contact with the ground. During *double stance*, all valves were in their default state for hip-hip reciprocal coupling and locked knees. Once the subject pressed the "go" button, the FSM transitioned to *early swing* phase where the knee mechanism was unlocked and the stimulation pattern initiated to swing the leg forward. The hips remained reciprocally coupled and the contralateral stance knee remained locked. When the ipsilateral hip flexion angle exceeded a predetermined threshold in *early swing* phase, the FSM transitioned to *late swing* phase. Once the ipsilateral knee exceeded an extension threshold, the knee locked in preparation for heel strike and *weight acceptance* phase. When the ipsilateral heel contact exceeded the FSR

[8] Chang SR, et al. "A stimulation-driven exoskeleton for walking after paraplegia," IEEE EMBS Conference, Orlando, FL, Aug 16-20, 2016.

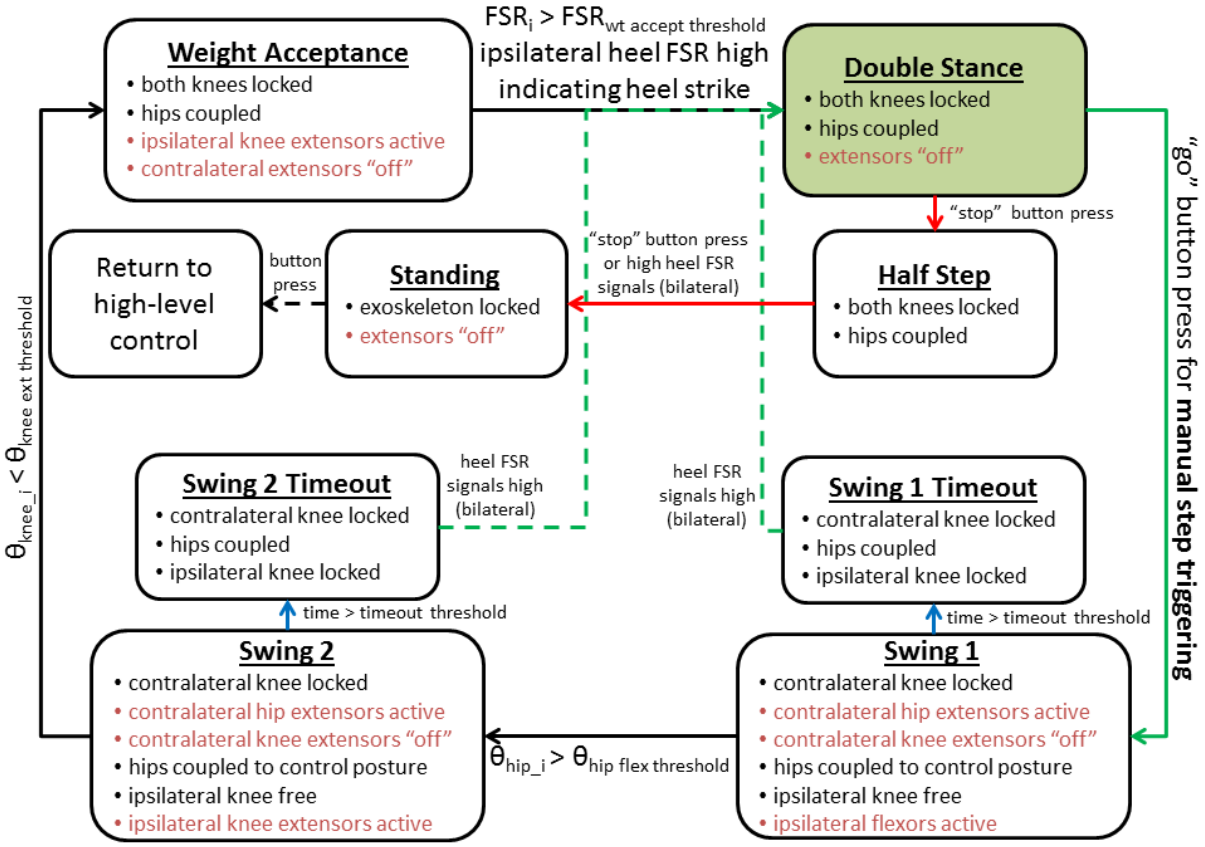

Figure 25. Gait event detector (GED) used in stepping state of FSM to transition user through gait pattern (green button press = "go" button; red button press = "stop" button, I = ipsilateral).

heel threshold, the FSM transitioned from *weight acceptance* to *double stance*. *Weight acceptance* phase ensured that the leg was loaded before the subject initiated another step. The subject then initiated the next step for the opposite leg by pressing the "go" button on the wireless finger switch. *Timeout* states were included into the GED for safety. The FSM transitioned to timeout states if the threshold was not reached within the duration of the step. The *timeout* state transitioned automatically back to *double stance* where the subject could initiate another step or exit the *stepping* state of the FSM by pressing the "stop" button to return to *standing* to initiate the *stand-to-sit* maneuver.

The GUI provided visualization of the hip and knee joint angles, the FSR signals, the valve states of the hydraulic circuits on the exoskeleton, the battery level, and the FSM current state (**Figure 26a**). The GUI also enabled data recording and manual adjustment of thresholds used in the GED and stimulation pattern lengths (**Figure 26b**). The time for a right or left step could be decreased/increased depending on subject preference for step duration. The GUI is a useful tool for FSM tuning, and data visualizing and recording.

Experimental procedure **-** The lengths of exoskeleton uprights were adjusted to the subject such that the hip and knee joint centers were aligned. The custom fitted AFOs fixed at neutral were attached to the uprights and either custom fitted or an off the shelf corset was attached to the adjustable pelvic band for exoskeleton-body coupling. For donning, the subjects transferred into the exoskeleton seated on a chair with uprights abducted. First, the feet were put into the shoes on the AFOs. Then the leg, thigh and abdominal Velcro straps were tightened and hip joints were adducted and locked before standing up. Subject assessment was along the 10m walkway within the motion capture space using the Vicon MX40 digital motion capture system (Vicon, Inc., Oxford, UK) in the Motion Study Laboratory at the Louis Stokes Cleveland Veterans Affairs Medical Center (**Figure 27**). Reflective markers were placed bilaterally on the subject's torso (sacrum, anterior superior iliac spine, and two vertically along the trunk on the corset), exoskeleton

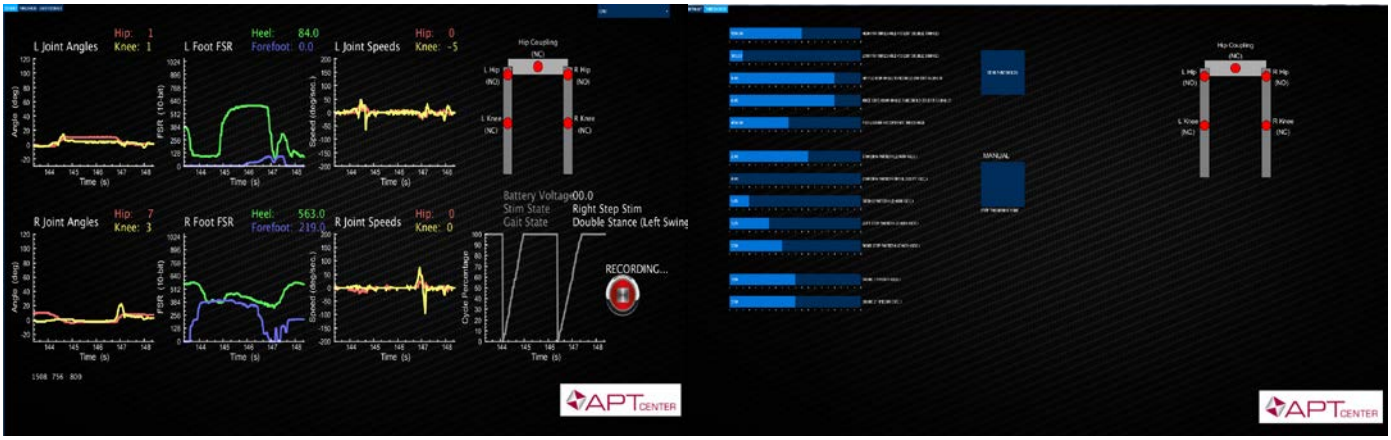

a) **b)**

Figure 26. a) GUI for visualizing and recording data and **b)** adjusting FSM parameters.

uprights (ankle/lateral malleolus joint center, two mid-thigh, and two mid-shank), and shoes (calcaneus, 2nd metatarsal head). Rotary encoders measured joint angles and FSR sensors recorded foot-floor contact.

The subject initiated standing by pressing the "go" button of the wireless finger switch. The hip and knee extensor stimulation ramped on during the sit-to-stand. Once in a good static upright posture, the subject pressed the "go" button to lock all joints and calibrate the exoskeleton sensors. The subject then initiated stepping by pressing the "go" button. Each subject walked at his preferred speed. During walking, the hips remained reciprocally coupled while the knees locked or unlocked depending on the state in the FSM (stance versus swing phase).

Hip and knee angles, FSR signals, and valve and state transitions were transmitted over Bluetooth and recorded on a portable tablet computer during walking. Sensor data was sampled at 50Hz and the motion capture data at 200Hz. Outcome measures included hip range of motion, peak knee angles, walking speed, and cadence.

Extensor muscle stimulation (standing and stance phase stimulation) remained "on" even when the exoskeleton joints were locked to compensate for poor coupling between the exoskeleton and the user's body (ex. knee sagging occurs when knee extensors are turned off). For Subject C, three trials were performed with modulation of the hip extensors (knee extensors remained on) in an attempt to give a boost to contralateral hip flexion using the hip-hip reciprocal coupling of the exoskeleton.

A typical progression through the gait cycle, joint angle and foot pressure data is shown in **Figure 28**. The horizontal lines in the figure indicate the threshold values to progress through a gait cycle. For example, the hip joint angle had to be higher than the threshold (blue) to transition from *early swing* to *late swing*. The vertical lines indicate transitions between the various states in the GED. *Double stance* state occurred at the orange vertical line and transitioned to the next state by button press. *Early swing* state (hip and knee flexion) is at the purple vertical line and transitioned when the hip flexion threshold was exceeded. *Late swing* state (hip flexion with knee extension) is the magenta vertical line and waited for a knee extension threshold to be achieved. *Weight acceptance* state occurred at the green vertical line with the heel FSR exceeding the set threshold. The summary of gait outcome measures for the three subjects evaluated is presented in **Table 6**.

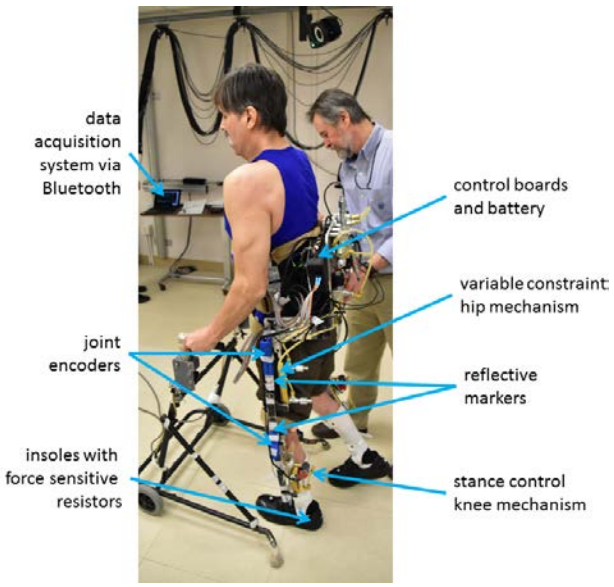

Figure 27. Experimental setup for SCI testing

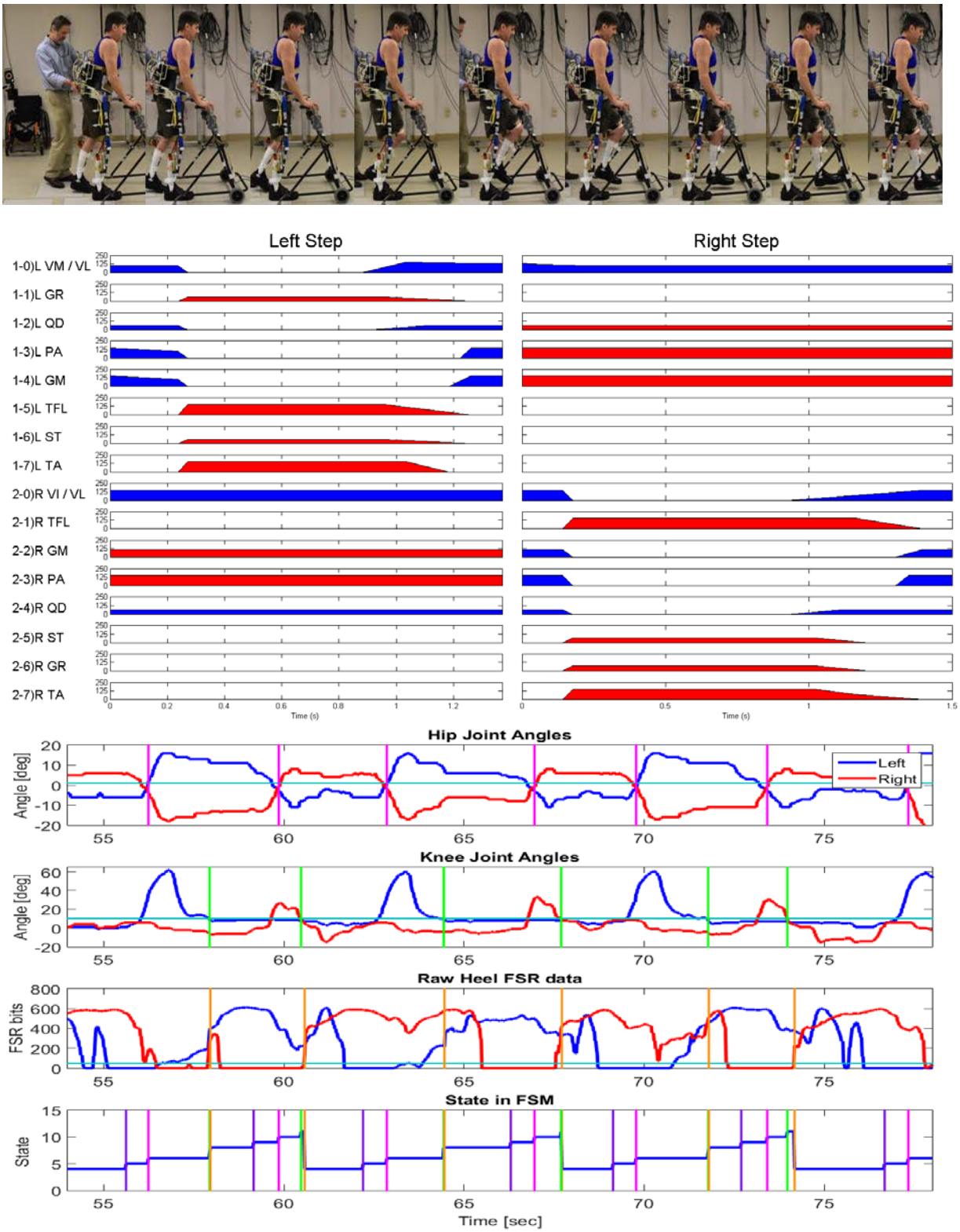

Figure 28. Shows (from top to bottom), a typical progression through the gait cycle, stimulation pattern of muscles driving the gait (as identified in Table 4), joint angle, foot pressure and controller state data for Subject A.

Table 6. Gait outcome measures

Subject	A	B	C
Hip Range of Motion [°]	39	21	29
Peak Left Knee Angle[°]	59.3 ± 2.2	8.0 ± 2.4	18.0 ± 2.9
Peak Right Knee Angle[°]	31.1 ± 2.4	19.4 ± 5.0	21.5 ± 5.0
Speed [m/s]	0.08	0.03	0.05
Cadence [steps/min]	18	10	14

Even with minimal controller tuning and no training, each subject was able to step with the HNP2 system. Achieving sufficient knee flexion during swing phase was a challenge in two out of three subjects and there were times when the forefoot would drag along the floor. However, the subject was still able to complete the step. Subjects B and C may have had difficulty in achieving sufficient knee flexion because they did not have electrodes implanted for specifically activating knee flexors. Surface stimulation of common peroneal nerve to elicit withdrawal reflex was added to Subject B's implanted muscle stimulation pattern for hip and knee flexion, and dorsiflexion. Subject C had experienced knee extensor stiffness which made it difficult to flex the knee. The poor foot-floor clearance resulted in the slower walking speed in this subject, along with the weight of the brace and passive resistance of hydraulics that had to overcome at the knee in the swing phase. The passive resistance of the hip hydraulic circuitry made it difficult to achieve sufficient and consistent hip flexion thus limiting step length.

Further development and testing would include turning off or reducing the duty cycle of the stance leg stimulation. With stimulation turned off and the knee locked during stance, the time to fatigue should extend.

KEY RESEARCH ACCOMPLISHMENTS:

- Hydraulic hip-knee coupling mechanism was designed, prototyped, tested and characterized for passive resistance and coupling ratio.
- Developed algorithm to optimize cylinder mounting for a 3 bar linkage transmission at the hip and knee to meet torque vs angle requirements specified for walking and stair climbing with HNP2.
- Designed, constructed and evaluated a new adjustable exoskeleton frame for ease of donning and doffing with attachments for customized corset and ankle foot orthoses. This included left and right leg uprights with abduction joints, pelvic band and hydraulic and electronic circuitry mounting frame.
- Designed and assembled a new variable constrained hip mechanism (VCHM2) and dual state knee mechanism (DSKM2) and characterized its passive resistance, compliance and locking torque.
- Instrumented exoskeleton with sensors to measure joint angles and foot pressure.
- Reduced total weight of the untethered HNP2 system by 18% from tethered HNP1 prototype.
- Developed Arduino based hardware for mobile computing platform for hybrid neuroprosthesis including embedded control board, signal conditioning board, and power supply.
- Designed software for mobile Arduino-based computing platform for control of muscle stimulation and hydraulic valves, data collection and analysis for HNP2.

- Designed software to run onboard finite state controller and stream real time data wirelessly to a PC/laptop for display and post processing.

- Designed wireless hand switch for user interface for function selection.

- Validated untethered operation of HNP2 in an able-bodied subject with onboard microprocessor running finite state controller.

- Untethered and self-contained HNP2 evaluated during gait in 3 subjects with SCI.

REPORTABLE OUTCOMES:

- **Manuscripts, abstracts, presentations:**

"A Hybrid Neuroprosthesis for Gait Restoration after Spinal Cord Injury"
April 13 2013, Research ShowCASE, Case Western Reserve University, Cleveland, OH.

"Coordinating the hip and knee joints during gait using a hybrid neuroprosthesis"
April 16, 2014, Musculoskeletal Research Day (Department of Orthopaedics), Case Western Reserve University, Cleveland, OH.

"Coordinating the hip and knee joints during gait using a hybrid neuroprosthesis"
April 18, 2014, Research ShowCASE, Case Western Reserve University, Cleveland, OH.

"Coordinating the hip and knee joints during gait using a hybrid neuroprosthesis"
May 22, 2014, VA Research Week, LSCDVAMC, Cleveland, OH.

Presented poster titled "Coordinating Hip and Knee Joints with A Hybrid Neuroprosthesis" at the 36th Annual International Conference of the Institute of Electrical and Electronics Engineers (IEEE) Engineering in Medicine and Biology Society (EMBC'14) in Chicago, IL.

Presented poster titled "Design of an Orthotic Mechanism to Control Stand-to-Sit Maneuver for Individuals with Paraplegia" at Research ShowCASE, Case Western Reserve University, Cleveland, OH (2015.04.17).

Oral presentation titled "Design of Orthotic Mechanisms to Control Stand-to-Sit Maneuver for Individuals with Paraplegia" at World Congress IUPESM (WC2015) in Toronto, Canada.

Chang SR, et al. (submitted 2016). "A stimulation-driven exoskeleton for walking after paraplegia," IEEE EMBS Conference.

To CS, Kobetic R, Bulea TC, Audu ML, Schnellenberger JR, Pinault G, Triolo RJ. Sensor-based hip control with hybrid neuroprosthesis for walking in paraplegia. *J Rehabil Res Dev*. 51(2)229-44, 2014.

Chang SR, Kobetic R, Triolo RJ. Understanding stand-to-sit maneuver: Implication for motor system neuroprosthesis after paralysis. *J Rehabil Res Dev.* 51(9):1339-1252, 2014.

Chang SR, Nandor MJ, Kobetic R, Foglyano KM, Quinn RD, Triolo RJ. Improving stand-to-sit maneuver for individuals with spinal cord injury. *Journal of NeuroEngineering and Rehabilitation*. 13:27, 2016.

Foglyano KM, Kobetic R, To CS, Bulea TC, Schnellenberger JR, Audu ML, Nandor MJ, Quinn RD, Triolo RJ. Feasibility of a Hydraulic Power Assist System for Use in Hybrid Neuroprostheses, *Applied Bionics and Biomechanics,* vol. 2015, Article ID 205104, 8 pages, 2015. doi:10.1155/2015/205104.

Nandor, Mark, Chang, Sarah, Kobetic, Rudi, Triolo, Ron, Quinn, Roger. "A Hydraulic Hybrid Nueroprosthesis for Gait Restoration in People with Spinal Cord Injuries." *Biomimetic and Biohybrid Systems: Living Machines, Edinburgh, 2016.* Ed. Lepora, N.F., Mura, A., Mangan, M., Verschure, P.F.M.J., Desmulliez, M., Prescott, T.J Springer International Publishing, 2016. Pg. 192 - 202.

- **Licenses applied for and/or issued;**
  US Patent Application Publication No.: US2014/0358053 A1,
  Pub Date: Dec 4, 2014.
  POWER ASSISTED ORTHOSIS WITH HIP-KNEE SYNERGY

- **Degrees obtained that are supported by this award;**
  - ***Opportunity for students to get involved in research***
    - Sarah Chang, M.S., graduate student, PhD., candidate in Biomedical Engineering
    - Mark Nandor, M.S., graduate student Ph.D., candidate in Mechanical Engineering
    - Lu Li, B.S., graduate student, M.S. candidate in Mechanical Engineering
    - Kiley Armstrong, undergraduate Mechanical and Biomedical Engineering student
    - Maria Lesieutre, undergraduate student majoring in Mechanical with minor in Biomedical Engineering.
    - Alexander Spalding, B.S., Mechanical Engineer
    - Theodore Frohlich, undergraduate student majoring in Biomedical Engineering

- **Funding applied for based on work supported by this award;**
  - Maria Lesieutre, applied and received SOURCE funding from CWRU to do summer research project on control of knee stiffness and damping for the stand-to-sit maneuver with HNP.
  - Sarah Chang, applied and received a training grant #: 5T32AR007505-28 from a Training Program in Musculoskeletal Research of the NIH. To pursue her graduate studies.
  - VA Merit Review to include power assist at the hip and knee as needed.

- **Employment or research opportunities applied for and/or received based on experience/training supported by this award**

  - Alexander Spalding, B.S.

Personnel	**Role**	**Percent Effort**
Ronald J. Triolo	Principal Investigator	10%
Musa L. Audu	Co-Investigator	10%
Roger Quinn	Co-Investigator	10%
Rudi Kobetic	Senior Engineer	10%
Mark Nandor	Mechanical Engineer	40%
John Schnellenberger	Electrical/Electronics Engineer	30%
Kevin Foglyano	Biomedical Engineer	10%
Lu Li	Computer/Software Engineer	50%
Dennis Johnson	Electronics Technician	10%

CONCLUSION:

The HNP2 designed, constructed and evaluated as part of this project is a significant improvement over the prototype HNP1 in terms of weight, autonomy, adjustability, and ease of use. The HNP2 combines exoskeletal structure with controllable hydraulic joints at the hips and knees for stability with neuromuscular electrical stimulation of paralyzed limbs to provide motive power for walking. Both systems are seamlessly integrated with a finite state machine controller using sensor-based gait event detector to coordinate stability and movement.

The exoskeletal structure is reconfigurable enough to accept commercially available or custom fabricated corsets and ankle foot orthoses for improved body-exoskeleton coupling. Similarly, the mobile computing platform is flexible enough to control stimulation with surface, percutaneous or implanted pulse generator stimulation, while the Arduino-based embedded controller can control valves in hydraulic mechanisms or be easily adapted for use with electric motors for power assist as needed for further development.

While significant reduction in weight was achieved with new hydraulic circuit design in HNP2, this came at the price of an increase in joint passive resistance. The proposed hydraulic hip-knee coupling mechanism was found not feasible for inclusion in the system due to high passive resistance and significant variability in coupling ratio placing unnecessary burden on the preserved neuromuscular system of the user. Instead, a spring assisted knee flexion was explored and recommendations are made for further development of motorized joint power assist and inclusion of additional muscle stimulation to increase hip and knee flexion and ankle plantar flexion to inject power for forward propulsion during push-off to improve speed and walking distance in individuals with SCI.

REFERENCES:

1. Kobetic R, To CS, Schnellenberger JR, Audu ML, Bulea TC, Gaudio R, Pinault G, Tashman S, Triolo RJ (2009). Development of hybrid orthosis for standing, walking, and stair climbing after spinal cord injury. *Jour Rehab Res and Dev* 46(3):447-462. DOI:10.1682/JRRD.2008.07.0087.
2. To CS, Kobetic R, Schnellenberger J, Audu M, Triolo RJ (2008). Design of a variable constraint hip mechanism for a hybrid neuroprosthesis to restore gait after spinal cord injury. *IEEE/ASME Transactions on Mechatronics*, 13(2):197-205.
3. To CS, Kobetic R, Bulea TC, Audu ML, Schnellenberger JR, Pinault G, Triolo RJ (2011). Stance control knee mechanism for lower-limb support in hybrid neuroprosthesis. *Journal of Rehabilitation Research & Development*, 48(7):839-850. DOI:10.1682/JRRD.2010.07.0135.
4. To CS, Kobetic R, Bulea TC, Audu ML, Schnellenberger JR, Pinault G, Triolo RJ (2012). Sensor-based stance control with orthosis and functional neuromuscular stimulation for walking after spinal cord injury. *J of Prosthetics and Orthotics*, 24(3):124-132.
5. To CS, Kobetic R, Bulea TC, Audu ML, Schnellenberger JR, Pinault G, Triolo RJ (2014). Sensor-based hip control with hybrid neuroprosthesis for walking in paraplegia. J Rehabil Res Dev. 51(2)229-44. http://dx.doi.org/10.1682/JRRD.2012.10.0190.
6. Bulea TC, Kobetic R, To CS, Audu M, Schnellenberger J, Triolo RJ (2012). A variable impedance knee mechanism for controlled stance flexion during pathological gait. *IEEE/ASME Transactions on Mechatronics*, 17(5):822-832. DOI:10.1109/TMECH.2011.2131148.
7. Bulea TC, Kobetic R, Audu ML, Triolo RJ (2013). Stance controlled knee flexion improves stimulation driven walking after spinal cord injury. Journal of NeuroEngineering and Rehabilitation, 10:68.
8. Bulea TC, Kobetic R, Audu ML, Schnellenberger JR, Triolo RJ (2013). Finite state control of a variable impedance hybrid neuroprosthesis for locomotion after paralysis. *IEEE Trans Neural Syst Rehabil Eng*. 21(1):141-51. doi: 10.1109/TNSRE.2012.2227124. Epub 2012 Nov 15. PubMed PMID: 23193320.
9. Winter DA. T*he Biomechanics and Motor Control of Human Gait: Normal, Elderly and Pathological*, 2nd ed. Waterloo: University of Waterloo Press, 1991.
10. Kobetic R, Marsolais EB (1994). Synthesis of paraplegic gait with multichannel functional neuromuscular stimulation. *IEEE Trans Rehab Eng.* 3(2): 66-79.
11. Chang SR, et al. (submitted 2016). "A stimulation-driven exoskeleton for walking after paraplegia," IEEE EMBS Conference.